Pressure Distribution Analysis of Fiber Reinforced Plastic Components Made by Rubber Pressure Moulding Technique

Kamal K. Kar,[1,2] S. D. Sharma,[2] P. Kumar,[1] J. Ramkumar,[1] R. K. Appaji,[3] K. R. N. Reddy[3]

[1]*Advanced Nano Engineering Materials Laboratory, Department of Mechanical Engineering, Indian Institute of Technology, Kanpur 208016, India*
[2]*Advanced Nano Engineering Materials Laboratory, Materials Science Programme, Indian Institute of Technology, Kanpur 208016, India*
[3]*Department of Mechanical Engineering, Kakatiya Institute of Technology and Science, Warangal, Andhra Pradesh, India*

Received 13 July 2006; accepted 20 March 2007
DOI 10.1002/app.26565
Published online 29 May 2007 in Wiley InterScience (www.interscience.wiley.com).

ABSTRACT: Fiber reinforced plastic component (FRP) having complex shaped geometry is prepared by rubber pressure molding (RPM) technique. The technique is based on the matching die set, where the die is made of hard metal like steel and the punch from flexible rubber like materials. The flexible rubber punch intensifies and uniformly redistributes pressure (both operating pressure and developed hydrostatic pressure due to the flexible rubber punch) over the surface of product. The distribution of pressure was analyzed by ANSYS over a processing pressure of 0.5–50 MPa. The analysis was extended to find out the optimum hardness of rubber mold, where the pressure distribution is uniform. For this, analysis was carried out for NR vulcanizates where the loading of carbon black was varied from 0 to 75 phr with an increment of 15 phr. The strain energy density function of 2-, 3-, 5- and 9 parameter Mooney-Rivlin; 1st-, 2nd-, and 3rd order Ogden; Neo-Hookean; 1st-, 2nd-, and 3rd order Polynomial; Arruda-Boyce; 1st-, 2nd-, and 3rd order Yeoh; and Gent were used. 45phr carbon black loading NR vulcanizate shows best result. © 2007 Wiley Periodicals, Inc. J Appl Polym Sci 105: 3333–3354, 2007

Key words: rubber pressure molding; fiber reinforced plastic (FRP); glass fiber; polyester resin; natural rubber; ANSYS

INTRODUCTION

Fiber reinforced plastic (FRP) components have been used for various types of equipment since the early 1950s. Its use has continued to grow in pulp and paper, power, waste treatment, semiconductor, metals refining, petrochemical, pharmaceutical, and other industries.[1–4] Even now it becomes a mainstream technology for the structural upgrade of concrete structures. Pressure vessels of all shapes and sizes, scrubbers, hoppers, hoods, ducts, fans, stacks, pipes, pumps, pump bases, valve bodies, elevator buckets, heat-exchanger shells and tube sheets, mist-eliminator blades, grating, floor coatings, and tank lining systems are just a few examples of products made of FRP. The chief reason for the popularity of these materials is their excellent high-strength and lightweight properties. In addition to these advantages another important characteristics of FRPs for structural repair and strengthening applications are their noncorrosive properties, speed, and ease of installation, lower cost, and esthetics. Several methods i.e., filament winding process, pultrusion method, vacuum bagging technique, autoclave technique, matching die set compression molding, resin transfer molding, etc have been developed to manufacture FRP products reported by Kelly and Zweben,[1] Agarwal and Broutman,[2] Hollaway,[3] Edwards,[4] and Kumar.[5] Among these, autoclave technique is a best method with respect to the less void content in the product, less standard deviation. In addition to this large sized product can be made easily using autoclave. But a major cost issue for manufacturing of FRP structures and parts using autoclave technique is the requirement of expensive tooling and disposable bagging materials. Additionally it requires long cure times, involves high energy consumption, volatile toxic byproducts, creates residual stress, and voids in the materials, and necessitates the use of expensive tooling capable of withstanding high autoclave temperature. It has been suggested that decreasing the manufacturing cost is a key step in increasing the overall usage of FRP products.

The conventional sheet forming process consist dies. Its basic requirement is large production rate,

Correspondence to: K. K. Kar (kamalkk@iitk.ac.in).
Contract grant sponsor: Ministry of Human Resource Development, New Delhi, India.

Journal of Applied Polymer Science, Vol. 105, 3333–3354 (2007)

otherwise the cost will be too high. However, the recent market requirements for products tend to vary quickly and to be of small volume, so the conventional sheet forming process with dies is not satisfactory. To adapt to the changing requirements of the market, the conventional process must be improved to form a flexible manufacture mode. Whereas the pressure forming process produces parts that are visually identical to the injection-molded parts. But it cannot be matched with the conventional injection molding's volume production capability, it easily achieves medium runs by the use of multiple-cavity tools. Generally it is used for giving a shape of thermoplastic material not for thermoset. Viscous pressure forming (VPF) is another forming process. It is developed on the basis of conventional flexible sheet forming technology, such as hydro-forming, and forming technology using an elastic body as the pressure-carrying medium, etc. It uses a kind of semisolid, flowable, and viscous materials as the pressure-carrying medium.[6]

The rubber pressure molding (RPM) technique for fabricating FRP laminates is a new development in manufacturing technology of thermoset composite materials (Fig. 1).[7–16] It is based on the matching die set, where the die is made of hard metal like steel and the punch from the flexible rubber like material. A split steel die and rubber punch were designed and fabricated to prepare the FRP product. The same split die was also used to cast the rubber punch. The use of flexible rubber punch applies hydrostatic pressure on the surface of the product. This RPM technique overcomes all difficulties of prevailing fabrication methods of complex shaped FRP components. Conventional process does not exert uniform pressure over the surface of product and loss of pressure is observed between component and die. It is difficult to prepare molds of intricate shapes. Even at higher curing pressure steel mold may not transfer uniform pressure over the complex shaped FRP components. It was found from experiment that the product made by RPM technique had void content less than 3%, free of delamination, and better bonding between fiber and resin.[7–16] Mechanical strengths like interlaminar fracture toughness, interlaminar shear strength, and tension test are better in RPM technique using appropriate rubber and hardness of rubber mold.[7–16] Another major advantage of FRP component made by RPM technique is less standard deviation of any properties.[7–16] The FRP specimens of glass fiber and epoxy resin prepared by RPM using butyl rubber with 45 phr loading of carbon black (N 330) have equal interlaminar fracture toughness, same or marginally higher (5%) interlaminar shear strength, slightly higher value (~ 10–13%) of tensile strength, modulus of elasticity, and strain% compared wiht the FRP specimen prepared by the conventional method.[7,8] When butyl rubber is replaced by natural rubber, interlaminar fracture toughness and interlaminar shear strength of FRP laminates decrease compared to the FRP specimen prepared by the conventional method without any change of tensile strength.[7,9] Whereas the FRP specimens prepared by RPM using silicone rubber have equal interlaminar fracture toughness and interlaminar shear strength compared to the specimens prepared by the conventional method.[7,10] In tension test, the FRP specimens have slightly higher value (~ 10%–13%) of tensile strength, modulus of elasticity, and strain%.[7,10] The FRP specimens made by RPM using polybutadiene rubber have lower (16%) interlaminar fracture toughness, lower (21%) interlaminar shear strength and slightly higher value of tensile strength, modulus of elasticity, and strain% compared to the specimen prepared by the conventional method.[7,11] In another experiment epoxy resin is replaced by polyester resin to see the performance of FRP laminates made by RPM technique.[7,12] Polyester resin is not cured in presence of rubber mold. To make it cure, rubber mold is coated with polyvinyl alcohol, polytetrafluoro ethylene, soap solution, silicone emulsion solution, etc.[7,13] However the performance of FRP laminates depends on the surface roughness. To understand its effect, in another study, FRP composites were made by RPM technique using rubber mold of different surface roughness.[14] The effect of temperature on interlaminar fracture toughness of FRP laminates made by RPM technique is reported by Sharma et al.[15] Since the hardness of rubber changes with the percentage of filler used in the rubber, Sharma et al.[16] discussed its effect on the properties of the FRP composites made by RPM technique. This was helpful in determining the optimum range of rubber composition/rubber hardness to produce good quality FRP products by RPM technique.

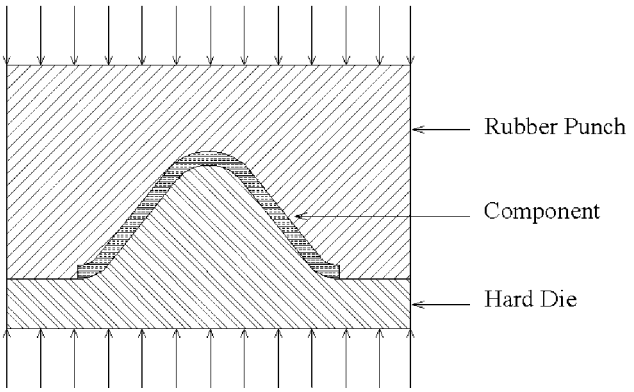

Figure 1 Concept of rpm technique.

These extensive studies suggest that the RPM technique produces a good quality complex shaped FRP components compared to the conventional tech-

TABLE I
Formulations of Natural Rubber Vulcanizates

Raw materials	A_0	A_{15}	A_{30}	A_{45}	A_{60}	A_{75}
Natural rubber (ISNR 10)	100	100	100	100	100	100
Zinc oxide	5.00	5.00	5.00	5.00	5.00	5.00
Stearic acid	3.00	3.00	3.00	3.00	3.00	3.00
Carbon black (N330)	0.0	15.0	30.0	45.0	60.0	75.0
Sulphur	5.00	5.00	5.00	5.00	5.00	5.00
TMTD	2.50	2.50	2.50	2.50	2.50	2.50

A_0, A_{15}, A_{30}, A_{45}, A_{60}, A_{75}: Suffix indicates loading of filler (phr: per hundred rubber).

nique.[7–16] But many fundamental questions appear to be unanswered. (1) The main hypothesis to get good quality FRP products using RPM technique is ''due to the uniform pressure distribution over the complex shaped product.'' Is it possible to verify this statement through finite element analysis? (2) Elastomer is hyperelastic material with a deformation more than 100%. Several phenomenological models like Arruda-Boyce, Mooney-Rivlin, Neo-Hooke, Ogden, Polynomial, Reduced polynomial, Van der Waals, Yeoh models, Gent, etc are available. Now the question is which strain energy density function is effective to verify the experimental data of stress-strain that will be used in finite element analysis. (3) Generally the FRP component is fabricated using RPM technique at a pressure of 0.65 MPa. Whether this pressure is sufficient/insufficient to get a good quality FRP components need to be answered. If it is insufficient what is the optimum pressure? (4) The hardness of rubber mold could be changed from 35 to 90 shore A by changing the composition of rubber mold. What should be the optimum hardness of rubber mold used in RPM technique to get good quality FRP product? The objectives of this article are to answer all these questions. The results are also compared with the corresponding values for the composites made by conventional method to evaluate the performance of RPM technique.

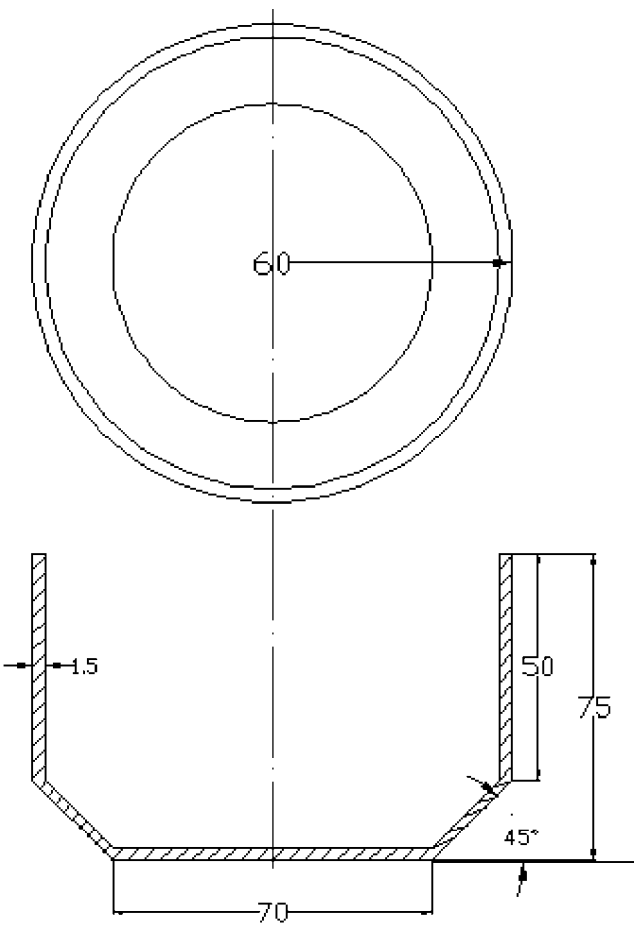

Figure 2 Product dimension.

EXPERIMENTAL

Raw materials

Glass fiber (E-glass, 4-satin) was used for this study supplied by Harsh Deep Industries, India. Unsaturated polyester resin (matrix), methyl ethyl ketone peroxide (curative), and cobalt octate (accelerator) were supplied by M/S Maypee Industries, Lucknow, India. S.R. Chemicals, India supplied natural rubber (ISNR 10). Natural rubber is cheaper than silicone/butyl/polybutadiene rubber. That's why it is used to

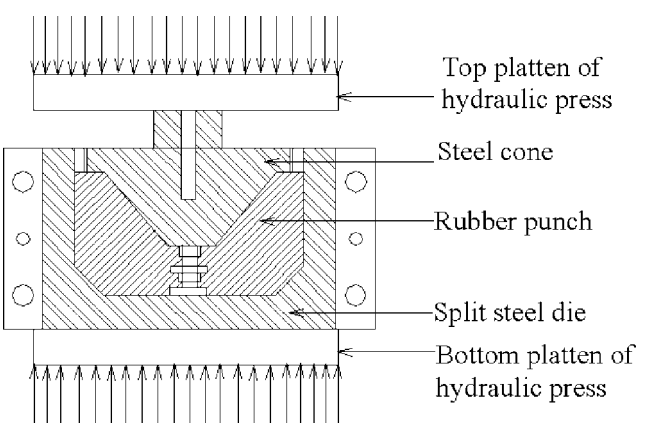

Figure 3 Setup for RPM technique.

Figure 4 FRP component. [Color figure can be viewed in the online issue, which is available at www.interscience.wiley.com.]

make a rubber mold in RPM technique. Other rubber chemicals like zinc oxide, stearic acid, accelerator (TMTD), sulfur (curing agent) and carbon black (N330) used to make the rubber mold were received from Avadh rubber limited, India.

Fabrication of rubber punch

The RPM technique is based on the matching die set, where the die is made of hard metal like steel and punch from flexible rubber like materials (Fig. 1). To fabricate a FRP product using RPM technique, a rubber punch is needed and prepared from NR. The strength of raw rubber is not sufficient to withstand the pressure applied during the fabrication of FRP components. To enhance its strength, other rubber chemicals like zinc oxide, stearic acid, sulfur, accelerator (TMTD), and carbon black, N330 (reinforcing filler) were used. The formulation used for this study to make the rubber mold is given in Table I.

Mixing of rubber chemicals

The compounding ingredients (rubber chemicals) were mixed with NR on a two roll mixing mill at a temperature of 25 to 50 °C and friction ratio of 1 : 1.1 according to the ASTM D 3182-89.[7,14]

Curing and molding

The curing characteristics of the mixed natural rubber were evaluated at a temperature of 150°C with a Rheometer *R*-100S according to ASTM D 2084-93. Subsequent molding for rubber punch was carried out in a hydraulic press at a temperature of 150°C for 40 min under a pressure of 5 MPa.[7,14]

Fabrication of FRP product

The complicated product selected in this study, which is a component of cooler pump, is usually made of steel sheet of thickness 1 mm. But it usually gets rusted and it is felt that a component of composite pump might be a more appropriate material choice. This component has three important geometry elements: (i) cylindrical, (ii) conical, and (iii) flat surface, and shown in Figure 2. The cylindrical part has an outer diameter of 120 mm and thickness of 1.5 mm; the conical portion has a half cone angle of 45° and thickness of 1.5 mm; the flat portion has a diameter of 70 mm and thickness of 1.5 mm. The total height of the pump cap is 75 mm. The glass fiber and unsaturated polyester resin were used to fabricate this component. Suitably cut pieces of glass fabric were stacked over the steel die by hand lay up technique. The steel die with preform and rubber punch were then loaded into a hydraulic press at a temperature of 25°C and a pressure of 1 MPa. After 24 h, the product was taken out and tested. This setup is shown in Figure 3. Figure 4 shows a FRP component made by the RPM technique. Five FRP components were made from each technique (RPM and conventional processes) to evaluate its performance in the structural applications. The void content, presence of delamination, fiber volume%, interlaminar fracture toughness, interlaminar shear strength, tensile strength, Young's modulus, etc were discussed elsewhere.[7–16]

Young's modulus measurement

Young's modulus of rubber specimen was measured from the initial slope (below 10% elongation) of the stress-strain curves in a Zwick UTM according to ASTM D-412-80 at a temperature of 25°C and strain rate of $9.5 \times 10^{-2}\ s^{-1}$. The Young's modulus for specimens A_0 to A_{90} (as per Table I) is given in Table II.

Hardness measurement

Shore A durometer was used to measure the hardness of rubber vulcanizates. The instrument used a

TABLE II
Young's Modulus and Hardness of Natural Rubber Vulcanizates

Vulcanizate number	A_0	A_{15}	A_{30}	A_{45}	A_{60}	A_{75}
Young's modulus (MPa)	2.6 ± 0.1	3.7 ± 0.1	8.6 ± 0.2	13.0 ± 0.2	15.5 ± 0.2	20.2 ± 0.2
Hardness (Shore A)	50 ± 1	61 ± 1	69 ± 1	72 ± 1	79 ± 2	85 ± 2

A_0, A_{15}, A_{30}, A_{45}, A_{60}, A_{75}: Suffix indicates loading of filler (phr: per hundred rubber).

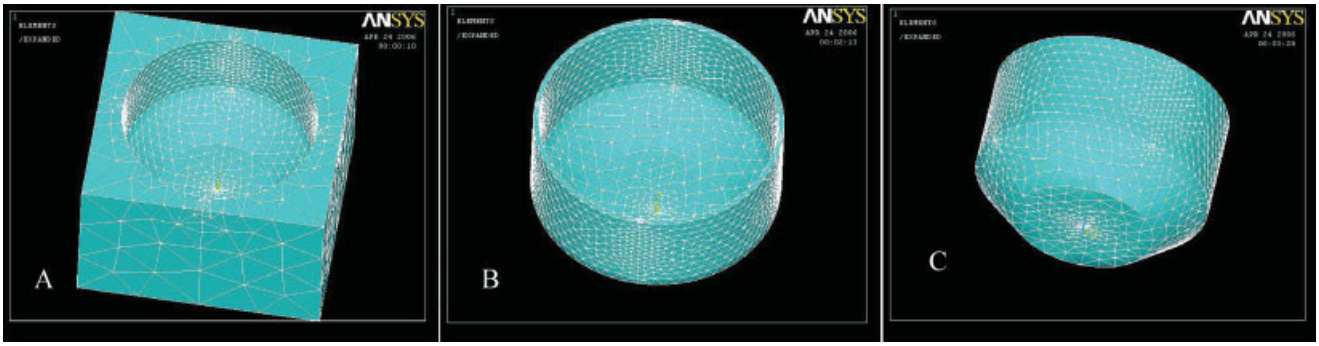

Figure 5 (A) Bottom mold; (B) FRP component; (C) Top mold (Rubber). [Color figure can be viewed in the online issue, which is available at www.interscience.wiley.com.]

calibrating spring to provide the indenting force. The load imposed by the spring varies with indentation. Reading was taken after 30 s of the indentation when firm contact had been established with the specimen. The method adopted is the same as that of ASTM D2240-81. Table II summarized the hardness value of rubber vulcanizates. The hardness of metal was measured by Rockwell hardness tester at 25°C according to ASTM E18-05e1 (B scale). The value is 82 HRB.

RESULTS AND DISCUSSION

The advantages of RPM technique are uniform pressure distribution over the complex shaped product and higher transmitted pressure, i.e., 81–82% pressure is transmitted to the FRP component, which indirectly helps to reduce the void content in FRP product. To understand how the pressure is distributed during processing of complex shaped geometry, an in-depth pressure distribution analysis is carried out by ANSYS (version 7) using the definition of nonlinear and contact type in eight steps, as follows: Step 1, part modeling; Step 2, material modeling; Step 3, assembly of the part and material modeling; Step 4, step modeling; Step 5, interaction modeling; Step 6, boundary conditions; Step 7, mesh modeling; and Step 8, job modeling.

Different parts i.e., bottom mold, FRP component, and steel punch/rubber punch are made according to the dimensions given in Figure 2 and shown in Figure 5. There are three different material types; steel is linear elastic isotropic, rubber is nonlinear and hyperelastic, FRP component is linear, elastic, and orthotropic. The reference point is used to apply boundary condition, initial condition, forces/pressures, etc. Any condition applied to the reference point is applied to the whole rigid body. The properties of the above materials are defined as: Steel: it is known as elastic material having a Young's modulus of 210 GPa and Poisson's ratio of 0.3. FRP component is defined as orthotropic material having nine elastic constants. These are as follows: E_{11} = 16.2, E_{22} = 15.3, and E_{33} = 7.3 GPa; Poisson's coefficients

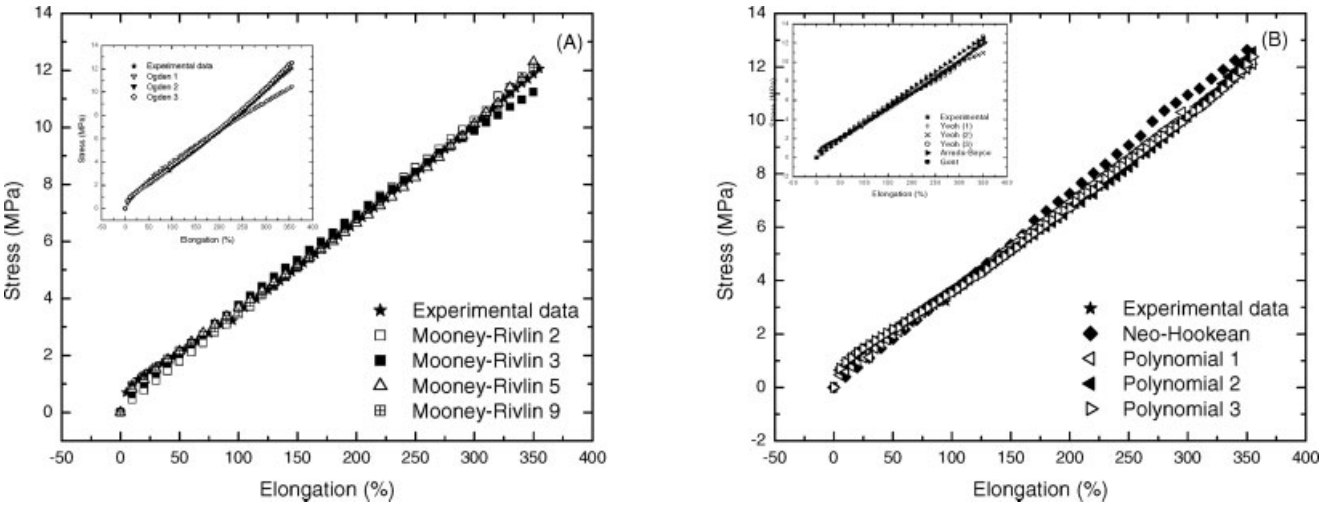

Figure 6 Experimental stress-elongation curve of NR vulcanizates containing 45 phr carbon black and its comparison with 2-, 3-, 5-, and 9 parameter Mooney-Rivlin A: 1st-, 2nd-, and 3rd order Ogden (inset of A); Neo-Hookean B: 1st-, 2nd-, and 3rd order Polynomial; Arruda-Boyce (inset of B); 1st-, 2nd-, and 3rd order Yeoh (inset of B); and Gent (inset of B).

TABLE III
Material Constants of Various Strain Energy Density Function for A_{45} Rubber Vulcanizates

	C10	C01	C11	C20	C02	C30	C21	C12	C03
Mooney-Rivlin									
2 parameter	5.78	−5.86	–	–	–	–	–	–	–
3 parameter	4.80	−4.86	0.12	–	–	–	–	–	–
5 parameter	8.76	−8.89	2.17	−0.32	−0.50	–	–	–	–
9 parameter	17.19	−17.44	1730	−826.8	−922.9	−0.05	0.70	203.6	−113.7
Polynomial									
1st order	5.78	−5.86	–	–	–	–	–	–	–
2nd order	8.76	−8.89	2.17	−0.32	−4.50	–	–	–	–
3rd order	17.18	−17.44	1730	827	−923	−0.05	0.703	203.06	−113.7
Yeoh									
1st order	0.05	–	–	–	–	–	–	–	–
2nd order	0.04	0.17	–	–	–	–	–	–	–
3rd order	0.03	0.38	−0.009	–	–	–	–	–	–
Ogden	μ1	a1	μ2	a2	μ3	a3	d1	d2	d3
1st order	0.05	5.56	–	–	–	–			
2nd order	0.02	5.57	0.03	5.57	–	–			
3rd order	0.02	5.57	0.02	5.57	0.02	5.57	–	–	–
Neo-Hookean	0.047	–	–	–	–	–	–	–	–
Arruda-Boyce	0.07	1.44							
Gent	0.05	0.97							

v_{12} = 0.115, v_{13} = 0.115, and v_{23} = 0.3; and shear moduli G_{12} = 3.9, G_{23} = 2.8, and G_{13} = 3.9 GPa.[17] Rubber is defined as hyperelastic material. For defining hyperelastic material in the finite element analysis, it is necessary to know the strain energy density function. It is represented by 2-, 3-, 5-, 7-, and 9 parameter Mooney-Rivlin; 1st-, 2nd-, and 3rd order Ogden; Neo-Hookean; 1st-, 2nd-, and 3rd order Polynomial; Arruda-Boyce; Gent; and Yeoh. These are represented as:

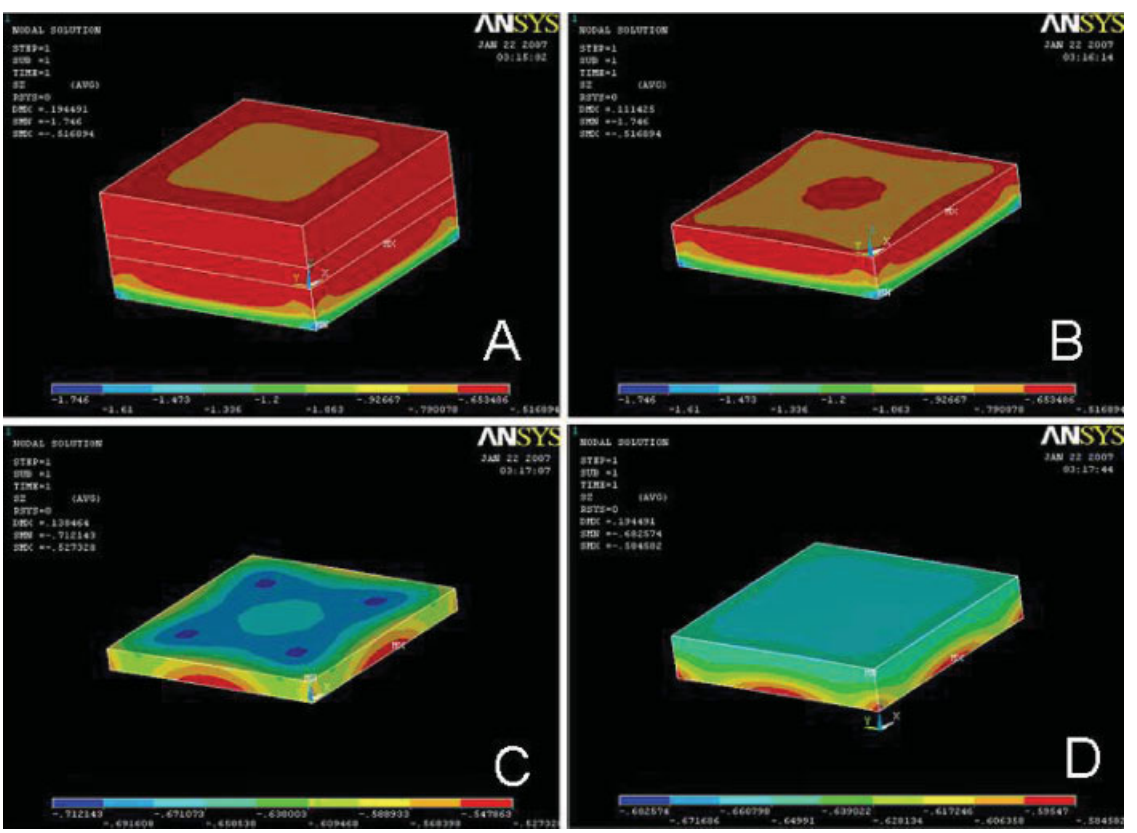

Figure 7 Pressure distribution diagram of a system where top, middle and bottom parts are made of rubber containing 45 phr carbon black. (A) assembly of top, middle and bottom parts. (B) top mold, (C) middle mold, and (D) bottom mold. [Color figure can be viewed in the online issue, which is available at www.interscience.wiley.com.]

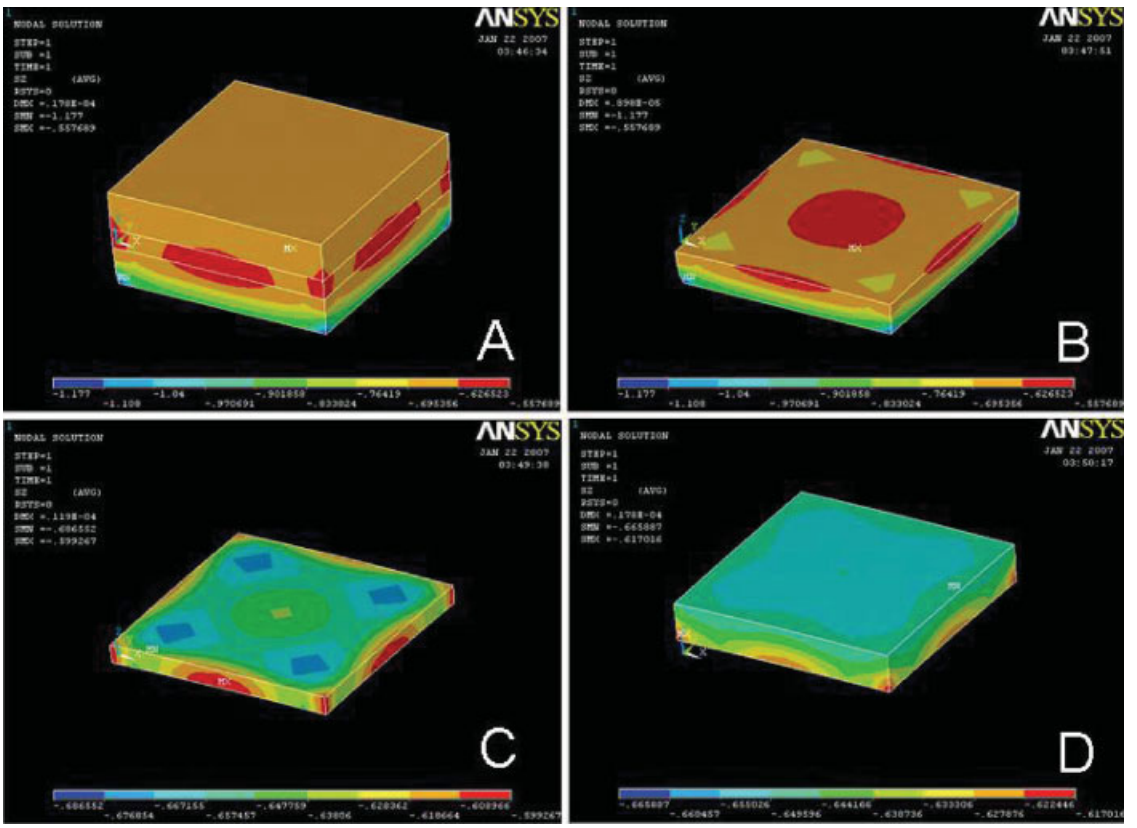

Figure 8 Pressure distribution diagram of a system where top, middle and bottom parts are made of steel. (A) assembly of top, middle and bottom parts. (B) top mold, (C) middle mold and (D) bottom mold. [Color figure can be viewed in the online issue, which is available at www.interscience.wiley.com.]

Mooney-Rivlin: The strain energy density function developed by Mooney is represented as[18]

$$U = \sum_{i+j=1}^{N} C_{ij}(I_1^c - 3)^i (I_2^c - 3)^j + \sum_{i}^{N} \frac{(J^c - 1 - R_t)}{D_i} \quad (1)$$

where U, C_{ij}, D_i, and R_t are strain energy density function, Rivlin's coefficients, material incompressibility and volumetric coefficient respectively. All other parameters are represented as

$$\begin{aligned} I_1^c &= (\lambda_1{}^c)^2 + (\lambda_2{}^c)^2 + (\lambda_3{}^c)^2, \\ I_2^c &= (\lambda_1{}^c\lambda_2{}^c)^2 + (\lambda_2{}^c\lambda_3{}^c)^2 + (\lambda_3{}^c\lambda_1{}^c)^2 \\ J^c &= \lambda_1{}^c\lambda_2{}^c\lambda_3{}^c \quad \text{and} \quad \lambda_i{}^c = \frac{\lambda_i}{(J^c)^{1/3}} \end{aligned} \quad (2)$$

Arruda-Boyce: Arruda-Boyce's strain energy density function is represented as[19]

$$U = \mu\left\{\frac{1}{2}(\bar{I}_1 - 3) + \frac{1}{20\lambda_m^2}\left(\bar{I}_1^2 - 9\right) + \frac{11}{1050\lambda_m^4}\left(\bar{I}_1^3 - 9\right) + + \ldots\right\} + \frac{1}{D}\left(\frac{J_{el}^2 - 1}{2} - \ln J_{el}\right) \quad (3)$$

where μ, λ_m, and D are temperature dependent material parameters. $\bar{I}_1$ is the first deviatoric strain invariant and defined as

$$\bar{I}_1 = \lambda_1^{-2} + \lambda_2^{-2} + \lambda_3^{-2} \quad (4)$$

where the deviatoric stretches are $\bar{\lambda}_i \;\; J^{-1/3}\lambda_i$. J is the total volume ratio. J_{el} is the elastic volume ratio as defined below in the ''thermal expansion'' and λ_i are the principal stretch. The initial bulk modulus and shear modulus are given by

$$\mu_0 = 2C_{10} \quad \text{and } K_0 = \frac{2}{D} \quad (5)$$

Neo-Hookean: The form of the Neo-Hooken strain energy density is[20]

$$U = C_{10}(\bar{I}_1 - 3) + \frac{1}{D_1}(J_{el} - 1)^2 \quad (6)$$

where C_{10} and D_1 are temperature dependent material parameters.

Ogden: Ogden represents the strain energy density function as[21]

$$U = \sum_{I=i}^{N} \frac{2\mu_i}{\alpha_i^2}\left(\bar{\lambda}_1^{-\alpha_i} + \bar{\lambda}_2^{-\alpha_i} + \bar{\lambda}_3^{-\alpha_i} - 3\right) + \sum_{i=1}^{N} \frac{1}{D_i}(J_{el} - 1)^{2i} \quad (7)$$

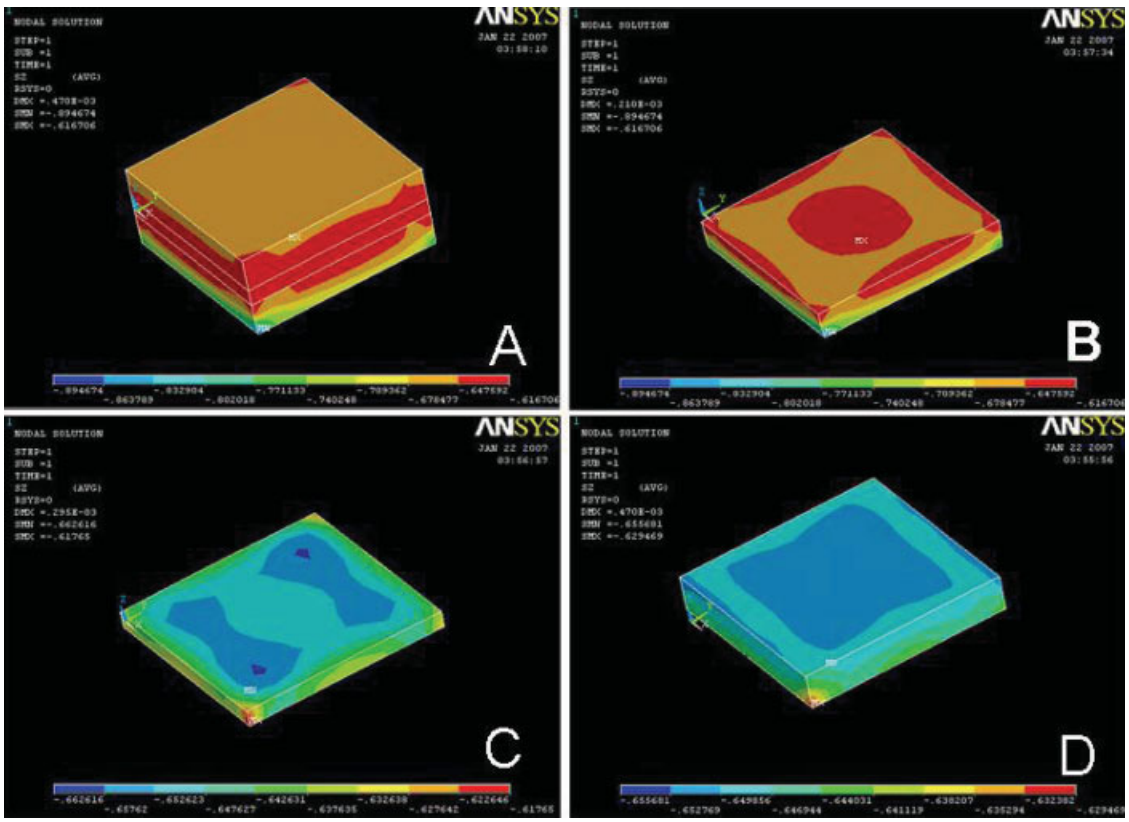

Figure 9 Pressure distribution diagram of a system where top, middle, and bottom parts are made of FRP. (A) assembly of top, middle and bottom parts. (B) top mold, (C) middle mold and (D) bottom mold. [Color figure can be viewed in the online issue, which is available at www.interscience.wiley.com.]

where μ_i, α_i, and D_i are temperature dependent material parameters.

Polynomial: The strain energy density is also represented in polynomial form as[22]

$$U = \sum_{i+j=1}^{N} C_{ij} \left(\bar{I}_1 - 3\right)^i \left(\bar{I}_2 - 3\right)^j + \sum_{i=1}^{N} \frac{1}{D_i} (J_{el} - 1)^{2i} \quad (8)$$

For cases, where the nominal strains are small or only moderately large (<100%), the first term in the polynomial series usually gives a sufficiently accurate result.

Yeoh: The strain energy density function of Yeoh is represented as[22]

$$U = C_{10} \left(\bar{I}_1 - 3\right) + C_{20} \left(\bar{I}_1 - 3\right)^2 + C_{30} \left(\bar{I}_1 - 3\right)^3 + \frac{1}{D_1} (J_{el} - 1)^2 + \frac{1}{D_2} (J_{el} - 1)^4 + \frac{1}{D_3} (J_{el} - 1)^6 \quad (9)$$

where C_{i0} and D_1 are temperature dependent material parameters.

Gent: the strain energy density function of Gent is represented by[23]

$$U = \frac{\mu J_m}{2} \ln \left(1 - \frac{\bar{I}_1 - 3}{J_m}\right)^{-1} + \frac{1}{d} \left(\frac{J^2 - 1}{2} - \ln J\right) \quad (10)$$

where μ is the initial shear modulus of material, J_m is the limiting value of $\bar{I}_1 - 3$. $\bar{I}_1$ is the first deviatoric strain invariant. J is the determinant of the elastic deformation gradient F. d is the material incompressibility parameter.

The stress strain data were calculated using the strain energy density function of 2-, 3-, 5-, 7-, and 9 parameter Mooney-Rivlin; 1st-, 2nd-, and 3rd order Ogden; Neo-Hookean; 1st-, 2nd-, and 3rd order Polynomial; Arruda-Boyce; 1st-, 2nd-, and 3rd order Yeoh; and Gent. These data are compared with the experimental stress strain data for natural rubber containing 45 phr carbon black (A_{45}) and shown in Figure 6. Mooney-Rivlin 3 parameter, 5 parameter, 7 parameter, and 9 parameter; Ogden 2nd, and 3rd orders; polynomial 1st, 2nd, and 3rdorders; Yeoh 2nd, and 3rd orders; Neo-Hooken; Arruda-Boyce fitted well with experimental data. But the Mooney-Rivlin 2 parameters, Ogden 1 order, Yeoh 1st order moderately fitted with experimental data. The material constants of the above models are calculated and used in the finite element analysis. These are summarized in Table III.

Before going to complex shaped product, the finite element analysis is carried out on the simple flat plate. Experimentally flat plates were prepared by

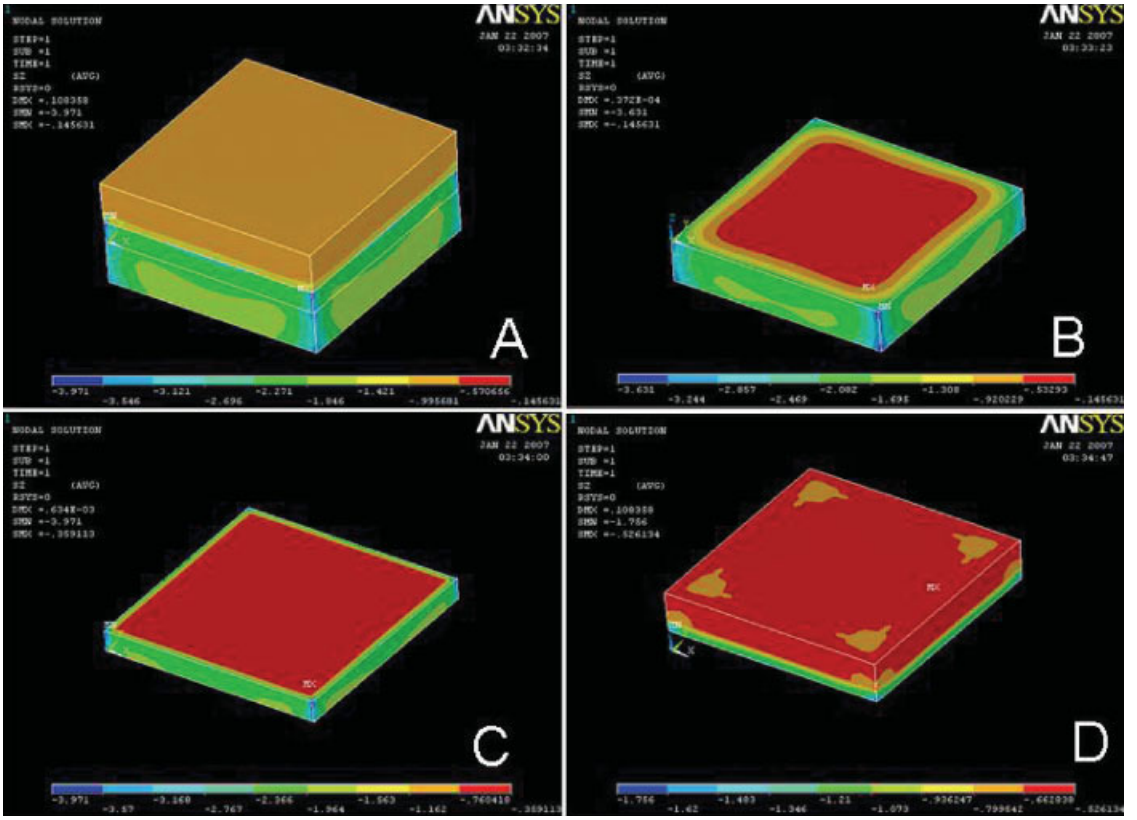

Figure 10 Pressure distribution diagram when the component is made by RPM technique. (A) assembly of top, middle and bottom parts. (B) top rubber mold, (C) middle FRP component, and (D) bottom steel mold. [Color figure can be viewed in the online issue, which is available at www.interscience.wiley.com.]

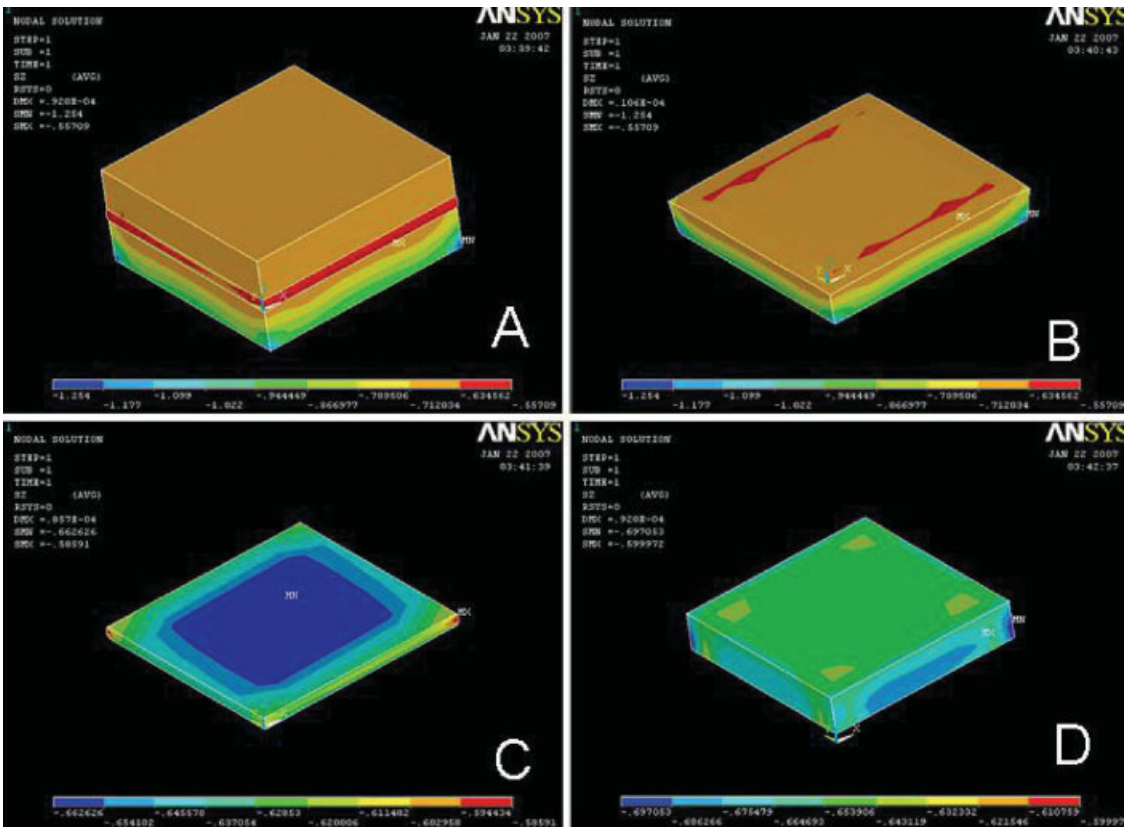

Figure 11 Pressure distribution diagram when the component is made by conventional technique. (A) assembly of top, middle and bottom parts. (B) top steel mold, (C) middle FRP component and (D) bottom steel mold. [Color figure can be viewed in the online issue, which is available at www.interscience.wiley.com.]

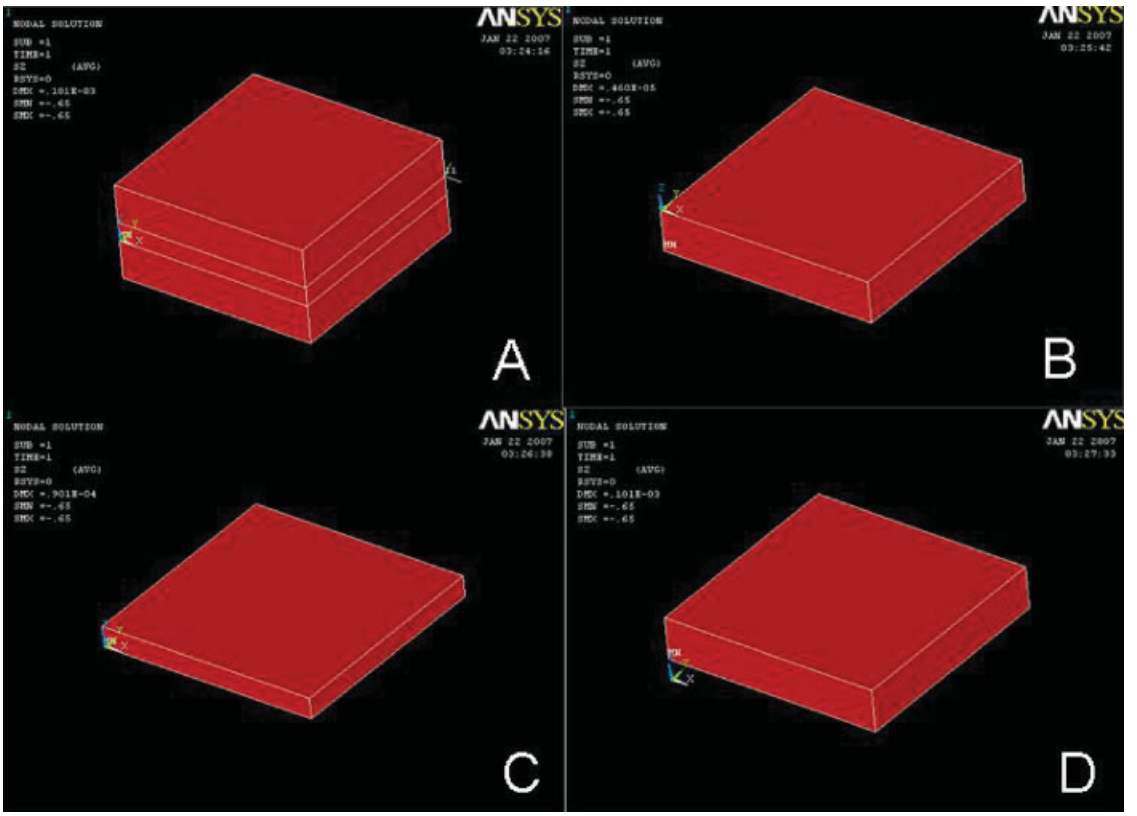

Figure 12 RPM molding technique; (A) both top (rubber), middle (FRP), and bottom (steel); (B) top rubber mold; (C) middle FRP component; (D) bottom steel mold. [Color figure can be viewed in the online issue, which is available at www.interscience.wiley.com.]

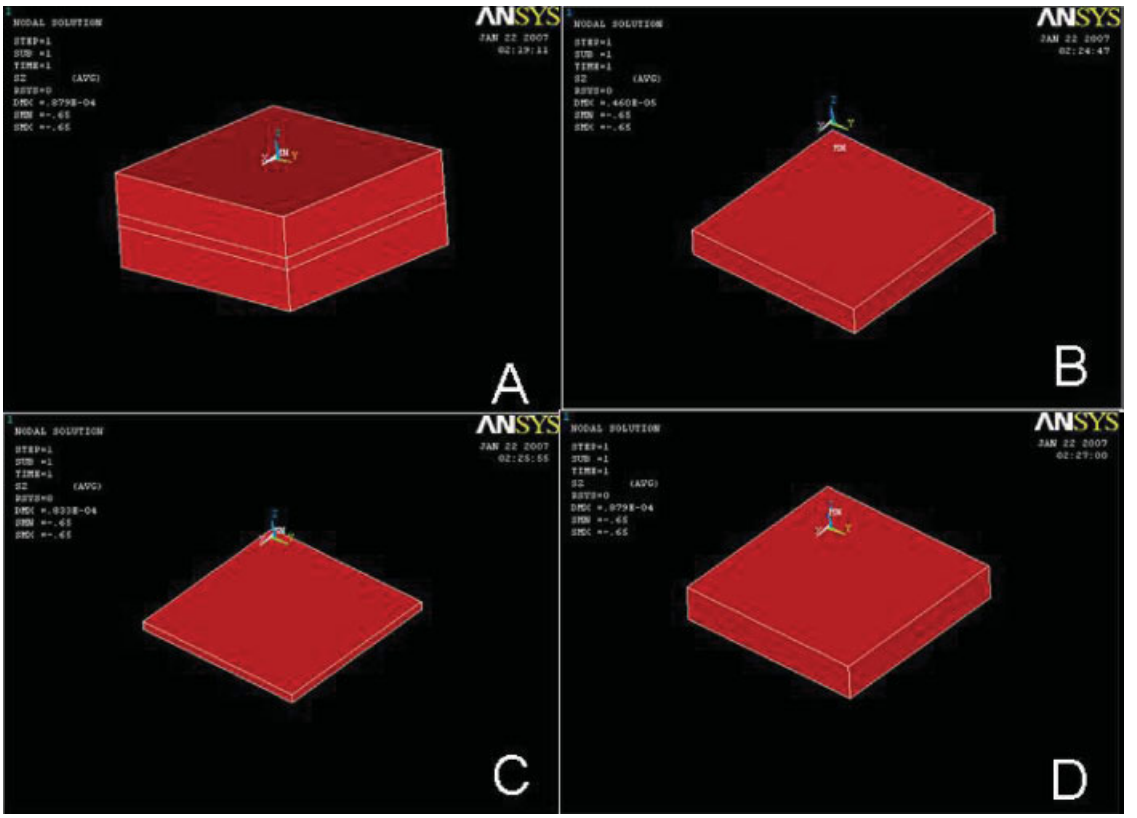

Figure 13 Conventional molding technique; (A) both top (steel), middle (FRP), and bottom (steel); (B) top steel mold; (C) middle FRP component; (D) bottom steel mold. [Color figure can be viewed in the online issue, which is available at www.interscience.wiley.com.]

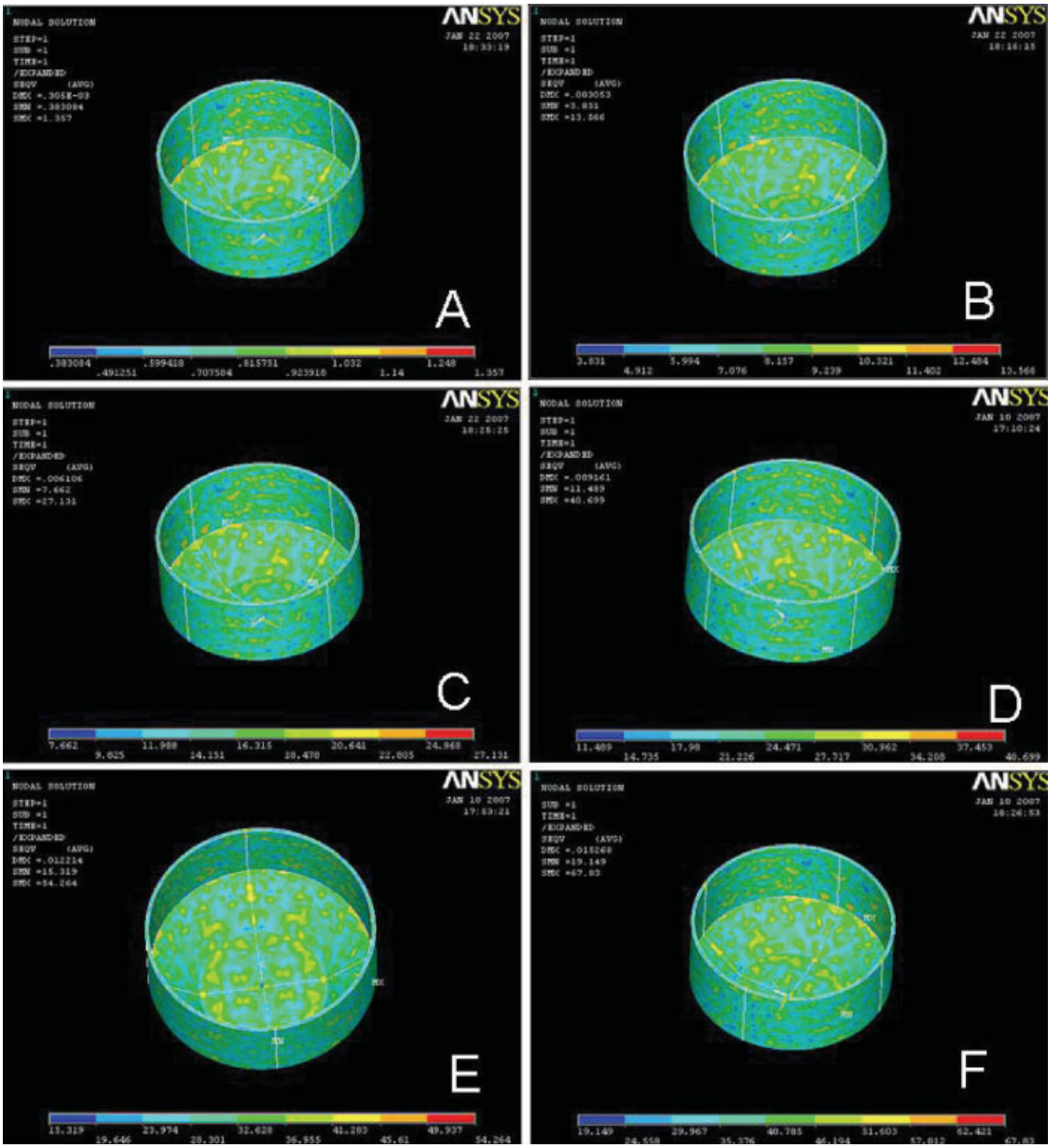

Figure 14 Pressure distribution on FRP component made by RPM technique where the rubber mold contains 45 phr carbon black. (Number inside parenthesis indicates applied pressure). (A) (1 MPa); (B) (10 MPa); (C) (20 MPa); (D) (30 MPa); (E) (40 MPa); (F) (50 MPa). [Color figure can be viewed in the online issue, which is available at www.interscience.wiley.com.]

both techniques. Specimens were also tested to know various parameters like voids, mechanical properties. RPM technique gives best results reported elsewhere.[7–16] To get better under standing of how the pressure is distributed over the component, finite element analysis is carried out using nine parameters Mooney-Rivlin strain energy density function (best fit to the experimental data compared to the other strain energy density function) at an operating pressure of 0.65 MPa for A_{45} rubber vulcanizates. The selection of 0.65 MPa pressure is due to the actual processing pressure used in earlier investigation to fabricate FRP components.[7–16] As 45 phr carbon black loading rubber mold shows best mechanical properties reported earlier[7,14] that's why it is used here. Top, middle, and bottom parts are made of rubber and it is a homogeneous structure. There are no constraints along the lateral directions means the only compressive stress of 0.65 MPa is applied vertically and the component deforms laterally. Figure 7 shows the pressure distribution of a system where top, middle and bottom parts are made of rubber containing 45 phr of carbon black loading. There is a variation of pressure from 0.69 to 0.63 and again it is

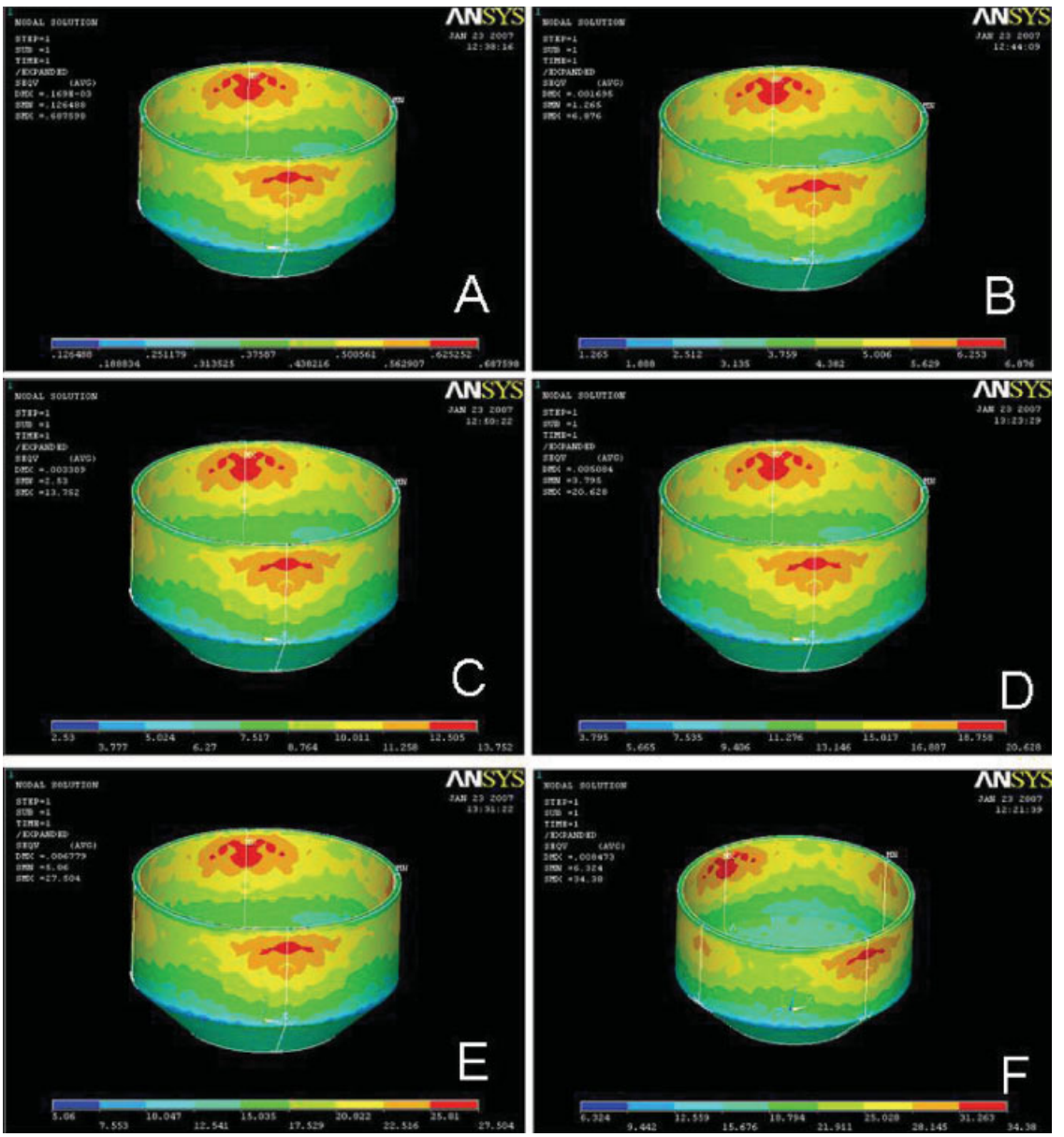

Figure 15 Pressure distribution on FRP component made by conventional technique. (Number inside parenthesis indicates applied pressure). (A) (1 MPa); (B) (10 MPa); (C) (20 MPa); (D) (30 MPa); (E) (40 MPa); (F) (50 MPa). [Color figure can be viewed in the online issue, which is available at www.interscience.wiley.com.]

varies from inner surface towards the outer surface in the same plane. This concentrated pressure as shown in Figure 7 is due to the gravitational force acting downwards. For validity of this model the analysis is carried out where the components are used as either steel or FRP (orthotropic). Figures 8 and 9 shows the pressure diagram for steel and FRP respectively. Same observations i.e., variation of pressure and concentric pressure are also observed here. The variations of pressure when all components are steel are 0.68–0.59 MPa whereas in case of FRP component it is 0.65–0.63 MPa. Now the analysis is extended to heterogeneous system where the top mold is made of rubber, middle is FRP, and bottom is steel, which is similar to the RPM technique. Figure 10 shows the pressure distribution diagram. The pressure is uniformly distributed over the FRP surface and slight variation is observed at the edge point. But the observed pressure on the FRP component is 0.76 MPa. It is much higher than applied pressure of 0.65 MPa. This 17% higher pressure is due to the developed hydrostatic pressure of the rubber mold. The observation that is excess pressure is not seen earlier when both top, middle and bottom parts are made of rubber. It is may be due to the low hardness of bottom mold (72 shore A, Table

II) as compared to the steel mold (82 HRB). The system i.e., bottom mold is not able to withstand this compressive pressure (0.65 MPa) when all these three parts are made of rubber as a result the bottom mold deforms accordingly and not shown any excess pressure. To verify the interesting results of 17% higher pressure in RPM technique, the analysis is carried out for conventional technique where top and bottom parts are made of steel and the middle component is made of FRP component. All other conditions are same as used earlier. The results are shown in Figure 11. The average pressure is 0.65, which is equal to that of applied pressure of 0.65 MPa. There is no excess pressure, which is observed in rubber mold of RPM technique. This is basically because of the absence of hydrostatic pressure of rubber mold developed during compression. Here the authors would like to mention that the actual process condition is slightly different from the above one. During the processing of FRP component only compressive pressure is applied vertically and there is no deformation in lateral direction. So in this context a constraint is applied i.e., no deformation in lateral direction. The analysis is carried out for RPM technique, where top, middle, and bottom parts are made of rubber, FRP and steel. And the results are shown in Figure 12. The pressure is uniformly distributed and exactly same to that of applied pressure of 0.65 MPa. Now the analysis is extended to the conventional technique, where top, middle and bottom molds are made of steel, FRP and steel respectively. The result is similar and shown in Figure 13. Exactly similar results are also observed for other analysis where all parts are made of either steel or rubber or FRP (Figures are not shown here).

Now the analysis is carried out for complex shaped product as shown in Figure 4 at the pressure of 1 MPa. The pressure profile for RPM technique is shown in Figure 14(A). It shows that pressure is uniformly distributed over the complex shaped geometry. It varies from 0.71 to 0.92 with an average of 0.81 MPa. To see how the pressure is distributed over the complex shaped product, the same analysis is carried out for the conventional technique and shown in Figure 15(A). The pressure is unevenly distributed over the surface and widely varies from 0.18 to 0.62 with an average of 0.40 MPa [Fig. 15(A)]. The maximum pressure is concentrated at the corner point, which is known as stress concentration zone. Also high pressure point is observed on the periphery of FRP component. This is may be basically because of the heterogeneous structure of FRP. The soft rubber mold evenly distributes this high pressure, which is not possible by the steel mold because of the rigid structure. Another important point authors would like to mention that the pressure transferred to the product is less in the case of conventional technique. The transmitted pressure is calculated as ''(average pressure/applied pressure) $\times$ 100%.'' At the pressure of 1 MPa, RPM technique transfers pressure $\sim$ 81% to the component, where as in case of conventional technique it is $\sim$ 40%. The excess pressure compared to the conventional technique, which is shown in RPM technique, is due to the hydrostatic pressure of rubber mold developed during the compression of rubber. Now the same analysis is carried out again at a pressure of 10 MPa for both the techniques. The pressure transferred to FRP component in RPM technique is 8.25 MPa [Fig. 14(B)], whereas in case of conventional technique it 4.06 MPa [Fig. 15(B)]. The pressure transferred in RPM technique is $\sim$ 82.5%, whereas in case of conventional technique it is $\sim$ 40.6%. And the variation of pressure in conventional technique is $\sim$ 1.88–6.25 MPa, where as in case of RPM technique it varies from 7.07 to 9.23 MPa. This supports the results, which is reported elsewhere,[7–16] i.e., less standard deviation of mechanical properties and improved mechanical properties using appropriate rubber and hardness of rubber mold.

The above analysis is carried out at a pressure of 1 and 10 MPa for A_{45} rubber vulcanizates. Now the analysis is extended over a wide range of pressure i.e., 0.5–50 MPa and want to see the pressure distribution over the product for both techniques. Few representative plots are shown in Figures 14 and 15 for RPM and conventional techniques respectively. In all cases of RPM technique, pressure is uniformly distributed over the surface of product, but the variation is observed in conventional technique. The results are shown in Figure 16. The transmitted pressure remains constant within 81–82% with increasing

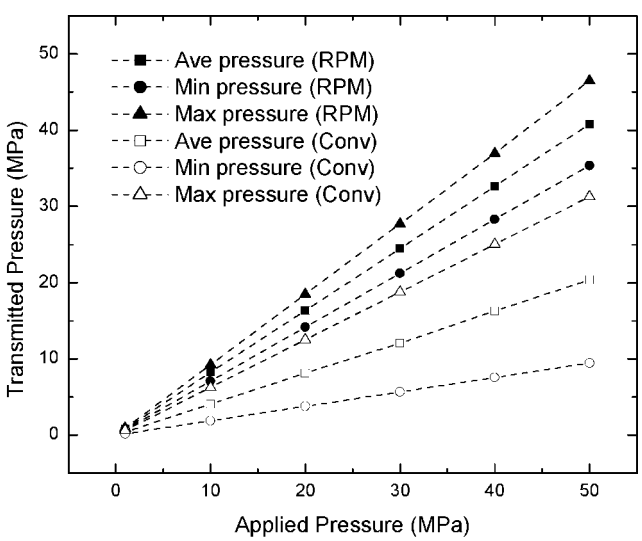

Figure 16 Applied pressure versus transmitted pressure for RPM and conventional technique.

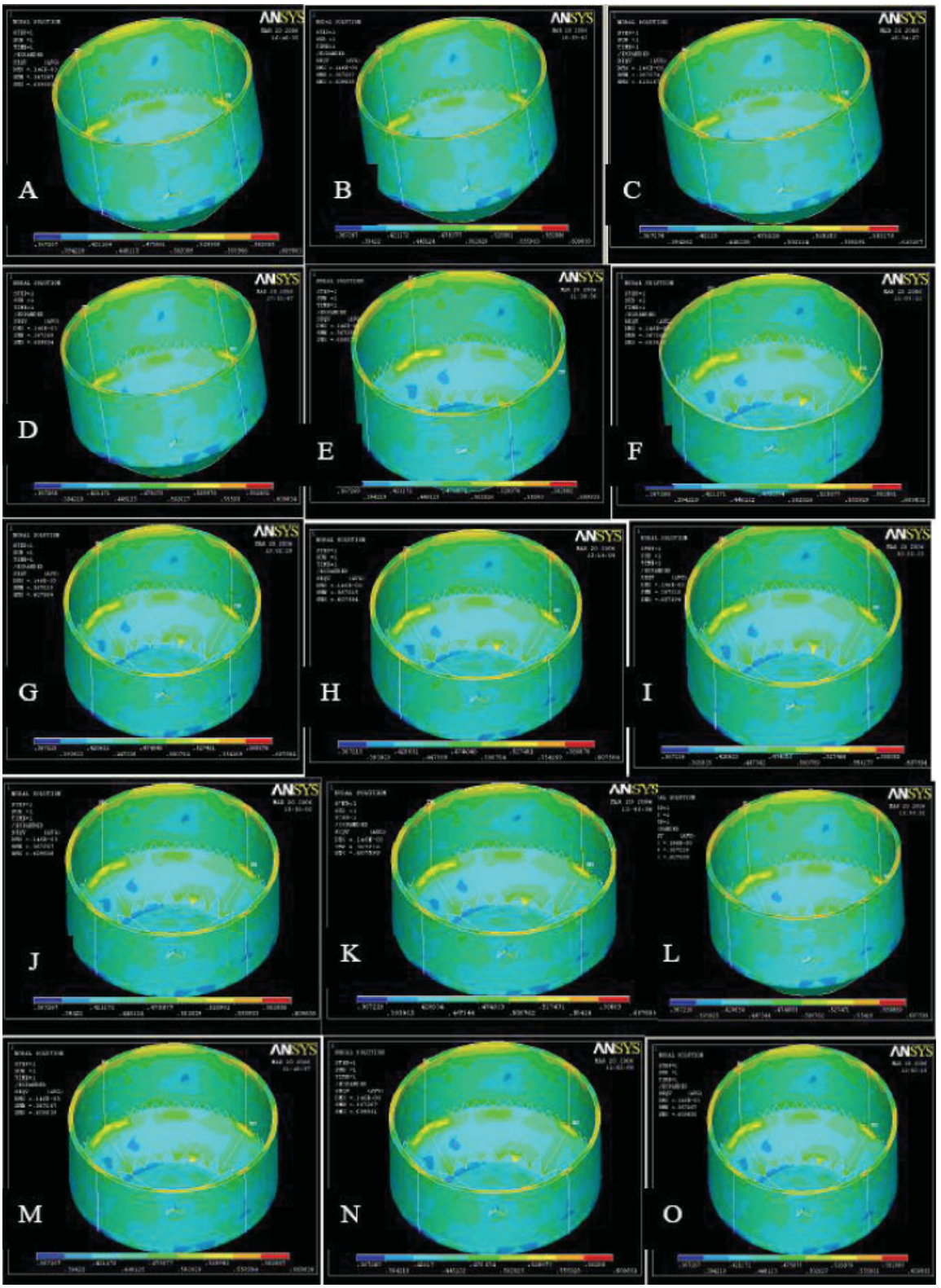

Figure 17 Pressure profile of flanged cone using various strain energy density functions. (A) Mooney (2), (B) Mooney (3); (C) Mooney (5); (D): Mooney (9); (E) Gent; (F) Neo-Hooken; (G) Ogden 1st order; (H) Ogden 2nd order; I: Ogden 3rd order; J: Polynomial 1st order; K: Polynomial 2nd order; L: Polynomial 3rd order; M: Yeoh 1st order; N: Yeoh 2nd order; O: Yeoh 3rd order. [Color figure can be viewed in the online issue, which is available at www.interscience.wiley.com.]

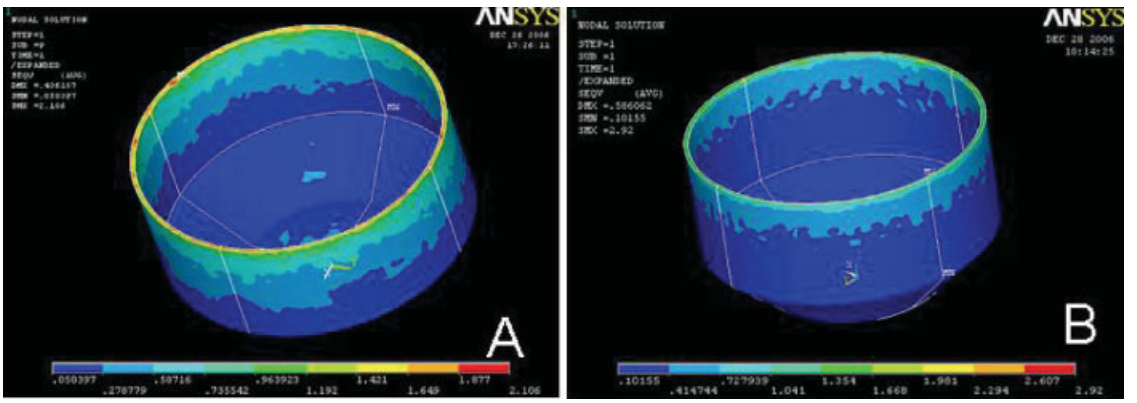

Figure 18 Distribution of pressure on FRP component made by RPM technique. A Poisson's ratio: 0.45 and B Poisson ratio: 0.40. Applied pressure on the top of rubber mold is 0.65 MPa. [Color figure can be viewed in the online issue, which is available at www.interscience.wiley.com.]

applied pressure from 1 to 50 MPa in the case of RPM technique, whereas in the case of conventional technique the transmitted pressure is ~ 40–41%. This proves that the RMP technique is a best technique to fabricate complicated shaped FRP component. This says that without changing the cross-sectional area, RPM technique produces more pressure to the FRP component compared to the conventional technique. In addition to this the pressure is uniformly distributed over the complex shaped product in the case of RPM technique.

Now the question arises bout the validity of other model equations i.e., Mooney-Rivlin 3 parameters, 5 parameters, 7 parameters, and 9 parameters; Ogden 2nd, 3rd orders; polynomial 1st, 2nd, 3rd orders; Yeoh 2nd, 3rd orders; Neo-Hooken; Arruda-Boyce, which shows good fitting to the experimental data of stress strain. The above analysis is carried out using 9 parameters Mooney-Rivlin strain energy density function for A_{45} rubber vulcanizates. To see the effect of other forms of strain energy density function on pressure distribution over the FRP surface 2-, 3-, 5- and 7 parameter Mooney-Rivlin; 1st-, 2nd-, and 3rd order Ogden; Neo-Hookean, 1st-, 2nd-, and 3rd order Polynomial; Arruda-Boyce; and 1st-, 2nd-, and 3rd order Yeoh are used. The pressure profile is shown in Figure 17. The pressure is uniformly distributed over the surface. Not significant difference is observed.

The Poisson's ratio used for rubber in the above analysis is 0.499. Now to see the effect of Poisson's ratio on the pressure distribution of FRP component, the analysis for 9 parameters Mooney-Rivlin strain energy density function is extended to 0.45 and 0.4 Poisson's ratio. The results are shown in Figure 18. The pressure is uniformly distributed over the complex shaped FRP component. As the Poisson's ratio is reduced from 0.499 to 0.45 and 0.40, the average pressure on the FRP component changes from 0.52 to 0.50 and 0.42 at the applied pressure of 0.65 MPa. As the Poisson's ratio is reduced, the transmitted pressure on the FRP component is also decreased. In addition to this the pressure is not uniformly distributed on the curved surface of FRP component. As

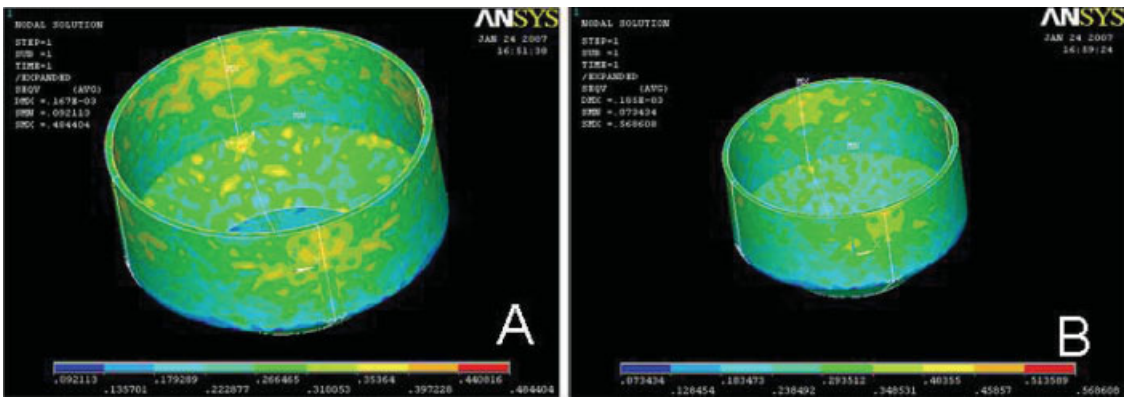

Figure 19 Effect of Poisson's ratio on pressure distribution of FRP component made by conventional technique. (A) 0.3 and (B) 0.0. [Color figure can be viewed in the online issue, which is available at www.interscience.wiley.com.]

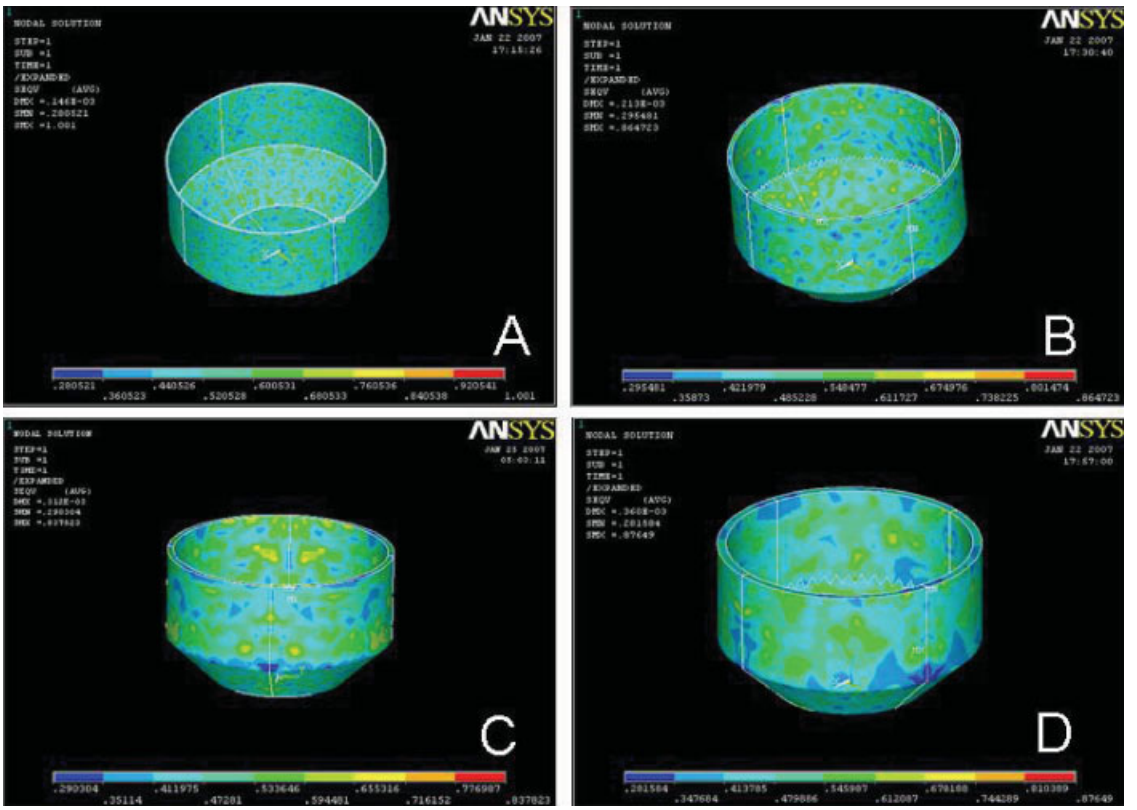

Figure 20 Effect of thickness of FRP components made by conventional technique on pressure distribution. (A) 1 mm, (B) 2 mm; (C) 3 mm, and (D) 4 mm thickness. [Color figure can be viewed in the online issue, which is available at www.interscience.wiley.com.]

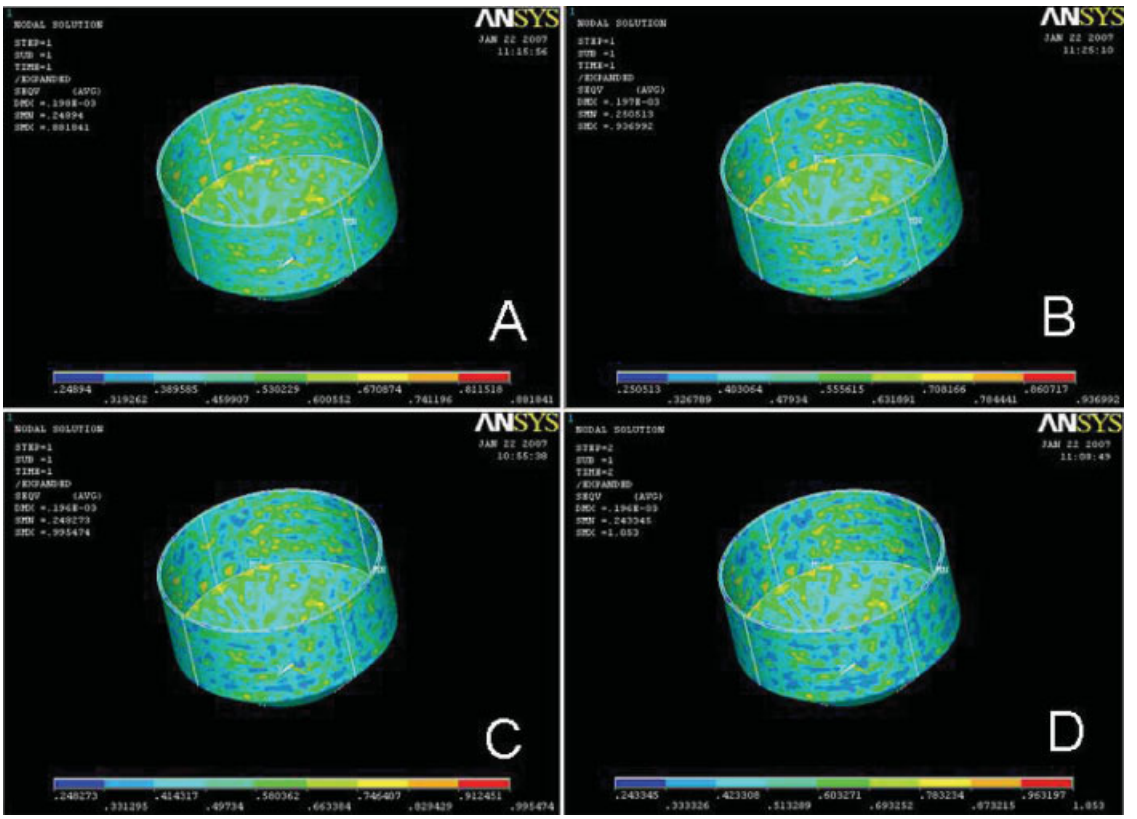

Figure 21 Effect of vol fraction of fiber in FRP component on pressure distribution of product made by RPM technique. The elastic constant E_{11} varies from 16 to 22 GPa. (A) 16 GPa, (B) 18GPa, (C)20 GPa, and (D) 22 GPa. [Color figure can be viewed in the online issue, which is available at www.interscience.wiley.com.]

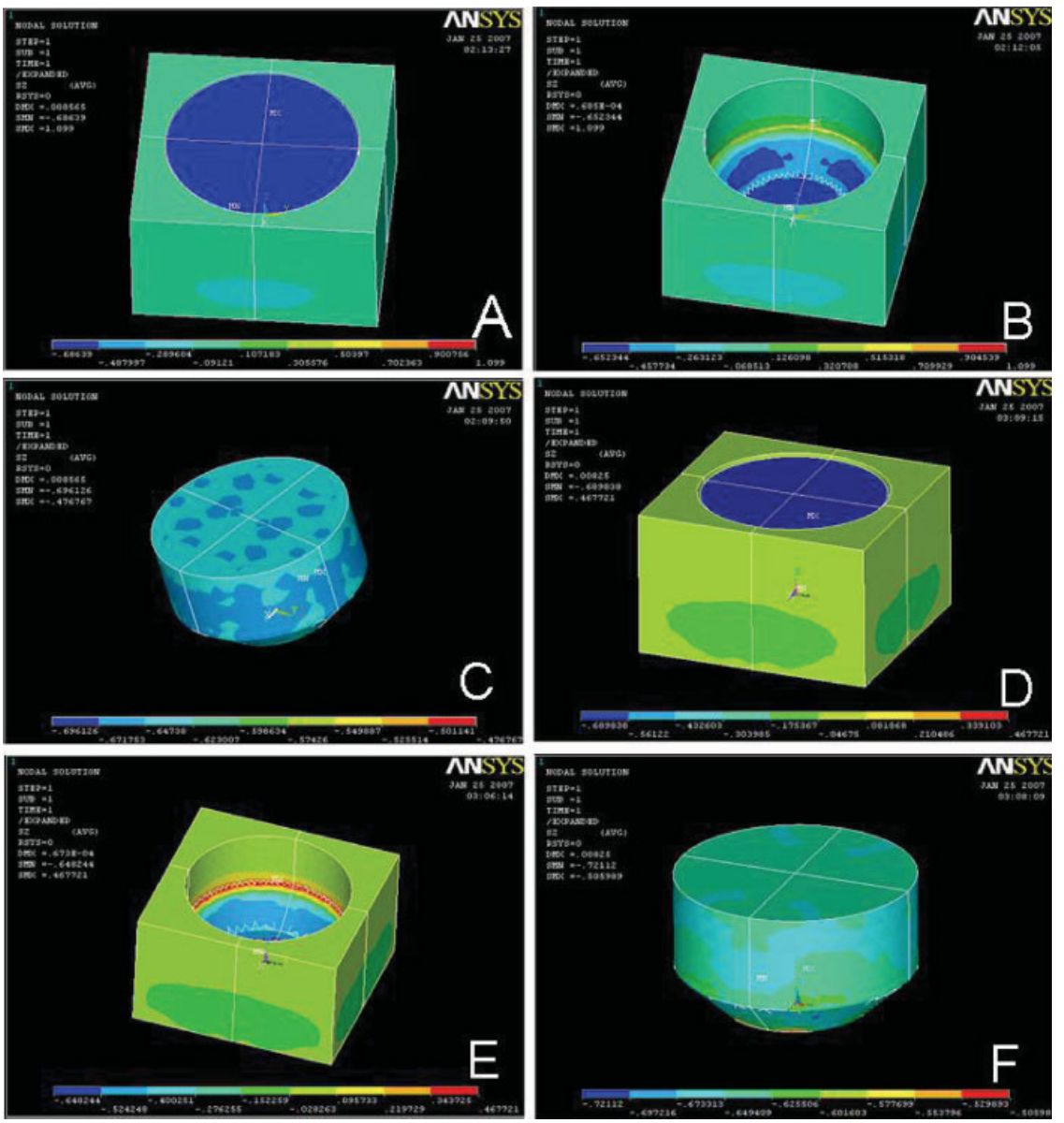

Figure 22 Pressure distribution in absence of FRP component. The gap between rubber mold and steel mold is varied. Gap 1 mm: (A), (B), and (C); Gap 2 mm: (D), (E), and (F). [Color figure can be viewed in the online issue, which is available at www.interscience.wiley.com.]

TABLE IV
Stress Components on Rubber and Steel Moulds in Absence of FRP Component

	On steel mould (MPa)	On Rubber mould (MPa)	
Stress component	Variation	Average	Variation
Gap between steel and rubber mould: 1 mm			
S_z	0.65–0.45	0.65	–
S_x	0.44–0.03	0.65	0.67–0.62
S_y	0.43–0.03	0.64	0.67–0.62
S_{eqv} (Equivalent stress)	0.38–0.53		0.93E-4–0.1E-3
Gap between steel and rubber mould: 2 mm			
S_z	0.65–0.52	0.65	–
S_x	0.43–0.02	0.65	0.67–0.62
S_y	0.46–0.08	0.64	0.67–0.62
S_{eqv} (Equivalent stress)	0.23–0.57	–	0.82 E-4–0.11E-3

The gap is varied from 1 to 2 mm.

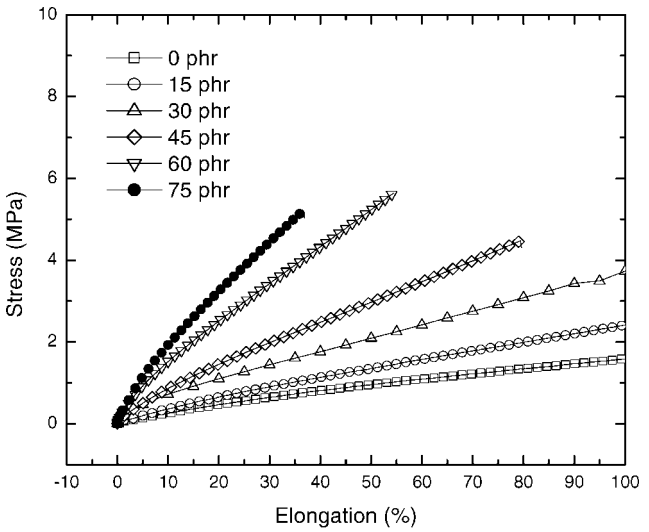

Figure 23 Experimental stress versus elongation curves of various NR vulcanizates. Experimental data were fitted with 9 parameters Mooney-Rivlin strain energy density function (continuous line).

for example at the Poisson's ratio of 0.499, the variation of pressure is 0.45–0.60 MPa, whereas in case of 0.45 and 0.40 Poisson's ratio the variations of pressure are 0.05–0.73 and 0.01–0.72 MPa respectively. Now the analysis is further extended to the zero Poisson's ratio. The system is unstable for rubber. But for the understanding purpose material properties of steel (Young's modulus of 210 GPa) are used. All other conditions are same. Only Poisson's ratio of 0 instead of 0.3 is used here. In addition to this top, middle, and bottom parts of the processing setup are steel, FRP and steel respectively. The pressure profiles for 0.3 and 0 Poisson's ratio are shown in Figure 19. The variations of pressure at the processing pressure of 0.65 MPa are 0.22–0.39 and 0.23–0.45 MPa for Poisson's ratio of 0.3 and 0 respectively. As such there is no difference of pressure distribution on the FRP component.

The question arises about the effect of thickness of FRP component on the pressure distribution. The thickness of FRP component used earlier is 1.5 mm. Now for better understanding the analysis is carried out for 1, 2, 3, and 4 mm thickness and the results are shown in Figure 20, when the component is made by RPM technique. The volume fraction of fiber in composite is constant. Only variable is the thickness of product. The dimensions of bottom mold, which are made of steel is same as that of earlier analysis. As the thickness of FRP component increases, to compensate this increased thickness, the dimensions of rubber mold are reduced accordingly. But the applied pressure is 0.65 MPa in all cases. All other boundary conditions are similar to that of earlier analysis. The pressure is uniformly distributed on the FRP component. The variations of pressure are 0.44–0.68, 0.48–0.62, 0.47–0.59, and 0.48–0.61 MPa for 1, 2, 3, and 4 mm thickness of FRP components respectively. The variation is very small. As such there is no remarkable effect of thickness of FRP component on pressure distribution during processing of FRP component through RPM technique. This indicates that FRP component of any thickness can be successfully made through the newly proposed RPM technique without loosing its quality. The same analysis is also carried out for conventional technique (pressure diagrams are not shown here). The results are similar to that of earlier one i.e., pressure is not uniform throughout the surface of FRP component. In addition to this as such there is no effect of thickness on pressure distribution on FRP component made by conventional technique.

Now an analysis is carried out to see the effect of fiber vol % on pressure distribution of FRP component. The thickness of FRP is constant. As FRP composites (45 vol %) are orthotropic materials having elasticity constants of $E_{11} = 16.2$, $E_{22} = 15.3$, and $E_{33} = 7.3$ GPa, Poisson's coefficients $\nu_{12} = 0.115$, $\nu_{13} = 0.115$, and $\nu_{23} = 0.3$ and shear moduli $G_{12} = 3.9$, $G_{23} = 2.8$, and $G_{13} = 3.9$ GPa.[17] These values are used in earlier studies. Now to address the above question i.e., the effect of vol % of fiber in FRP components on pressure distribution, there is a need of above nine materials

TABLE V
Comparison Between RMP and Conventional Techniques

Constant	A_0	A_{15}	A_{30}	A_{45}	A_{60}	A_{75}
$C1$	−0.376	−0.777	−1.187	17.185	−2.113	−3.128
$C2$	0.424	0.861	1.324	−17.445	2.364	3.511
$C3$	0.797	2.388	4.306	−826.847	7.740	12.108
$C4$	−2.056	−5.908	−10.526	1729.93	−18.883	−29.175
$C5$	1.536	4.139	7.223	−922.90	12.929	19.652
$C6$	−3.54e-11	1.86e-10	1.61e-9	−0.052	6.07e-9	1.49e-7
$C7$	5.14e-9	−3.25e-8	−2.12e-7	0.703	−7.18e-11	−9.64e-6
$C8$	−0.199	−0.597	−1.077	203.05	−1.935	−3.627
$C9$	0.215	0.581	1.016	−113.72	1.818	2.756

45 phr carbon black was used to make the rubber mould.

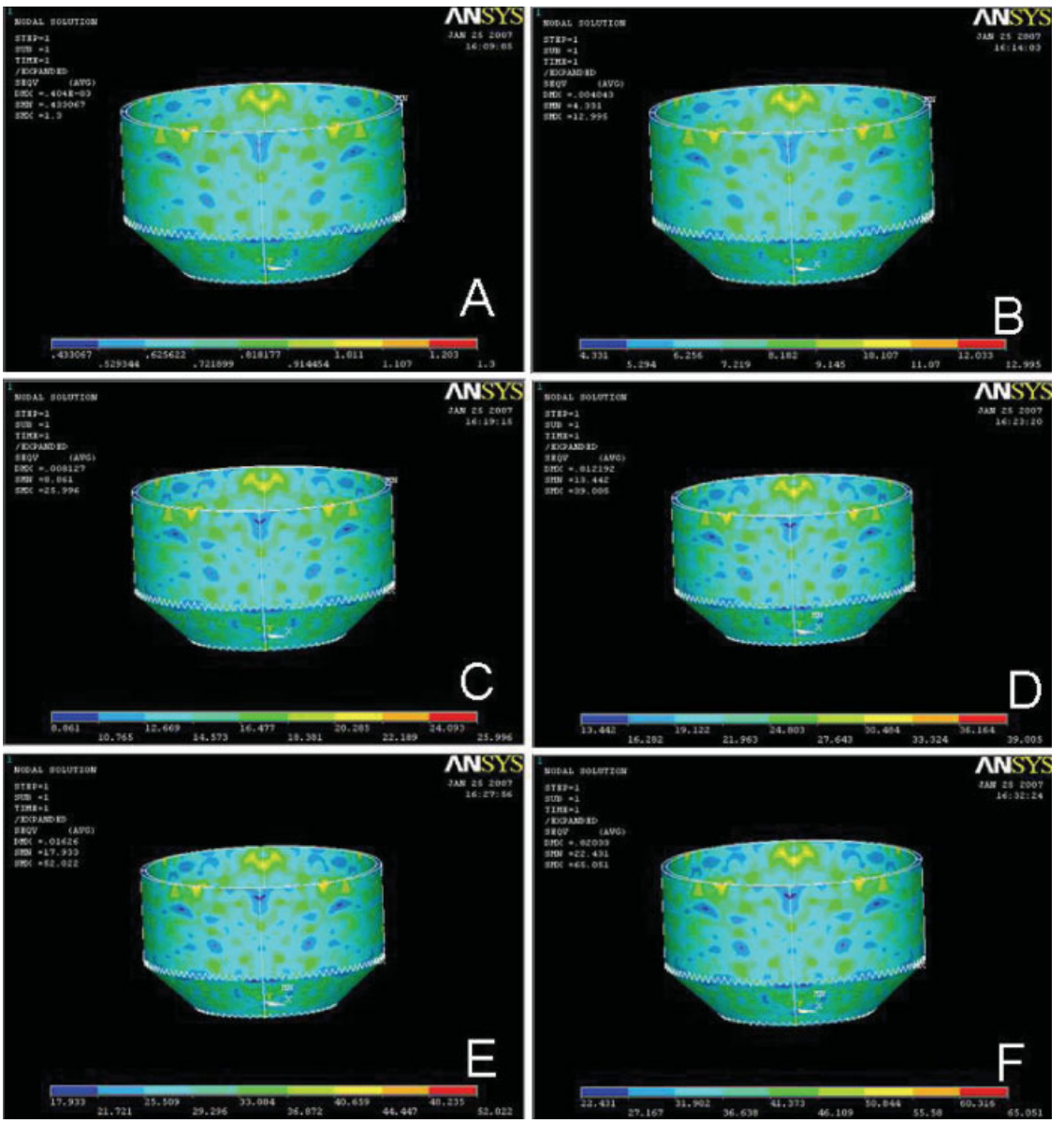

Figure 24 Pressure distribution on FRP component made by RPM technique where the rubber mold contains 0 phr carbon black. (Number inside parenthesis indicates applied pressure). (A) (1 MPa); (B) (10 MPa); (C) (20 MPa); (D) (30 MPa); (E) (40 MPa); (F) (50 MPa). [Color figure can be viewed in the online issue, which is available at www.interscience.wiley.com.]

constant as a function of vol fraction of fiber. Unfortunately systematic literature data is not available. But for understanding purpose, E_{11} values are varied from 16 to 18 to 20 to 22 GPa. All others parameters i.e., E_{22}, E_{33}, ν_{12}, ν_{13}, ν_{23}, G_{12}, G_{23}, and G_{13} are same as that of earlier one. The pressure diagram is shown in Figure 21. It varies from 0.45 to 0.60, 0.44 to 0.63, 0.44 to 0.66, and 0.42 to 0.69 MPa when the E_{11} is varied from 16.2 to 18, 20, and 22 GPa respectively. In all cases the pressure is uniformly distributed on the FRP component. In addition to this there is no remarkable effect of vol % of fiber in FRP component on pressure distribution. This suggests that FRP component of any vol fraction of fiber can be successfully made through the newly proposed RPM technique without loosing any product quality.

For better understanding an analysis is carried out in absence of FRP component to see the pressure distribution. The gap between bottom steel and top rubber mold is equal to that of the FRP component, which is 1.5 mm and used in earlier investigation. Now the gap between bottom steel mold and top rubber mold is varied from 1 to 2 and 3mm. It is filled by air. There is no displacement of air during compression when the processing pressure of 0.65 MPa is applied on the top of rubber mold. The

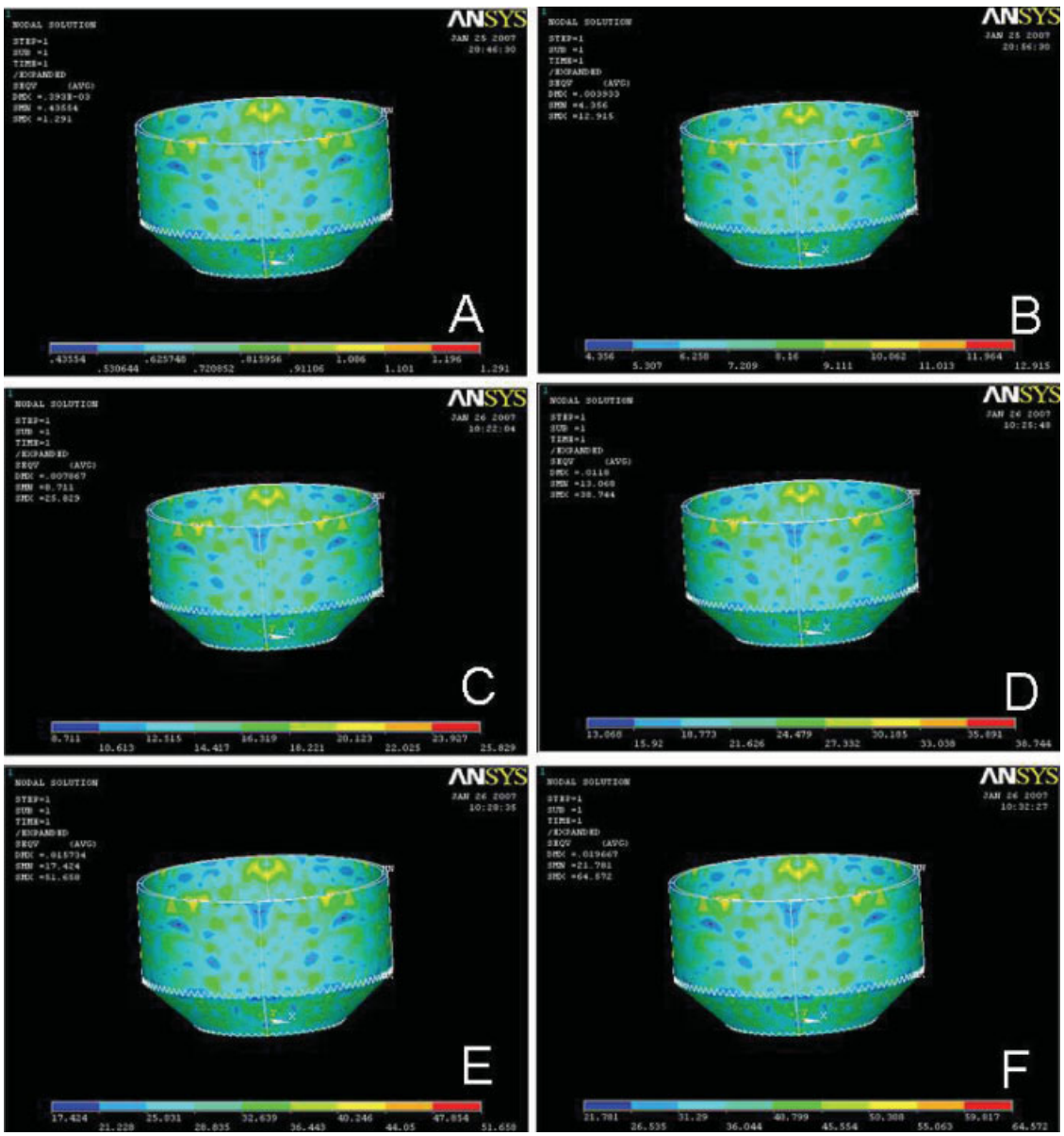

Figure 25 Pressure distribution on FRP component made by RPM technique where the rubber mold contains 60 phr carbon black. (Number inside parenthesis indicates applied pressure). (A) (1 MPa); (B) (10 MPa); (C) (20 MPa); (D) (30 MPa); (E) (40 MPa); (F) (50 MPa). [Color figure can be viewed in the online issue, which is available at www.interscience.wiley.com.]

results are shown in Figure 22 for 1 and 2 mm gap. The stress components are summarized in Table IV. Up to 2 mm gap there is no remarkable difference on pressure distribution on the rubber mold. The pressure is uniformly distributed throughout the surface. But at the gap of 3 mm, the peculiar pressure distribution is observed, which is not included here (need more detailed investigation).

RPM technique shows that the pressure is uniformly distributed over the product and $\sim$ 82% of the applied pressure is transferred to the FRP component during processing of FRP components. As the RPM technique uses a rubber mold, now the question arises about the optimum hardness of rubber mold, where the pressure distribution should be uniform and the transmitted pressure should be as max as possible. At the same time processing pressure should be minimum. To find out the answer an in-depth analysis is carried out for RMP technique, where the hardness of rubber mold varies from 50 (0 phr carbon black loading) to 85 shore A (75 phr carbon black loading) and the applied pressure is varied from 0.5 to 50 MPa. Stress-strain data are also measured for other compositions as per formulation given in Table I and shown in Figure 23. As Mooney-Rivlin 3 parameters, 5 parameters, 9 param-

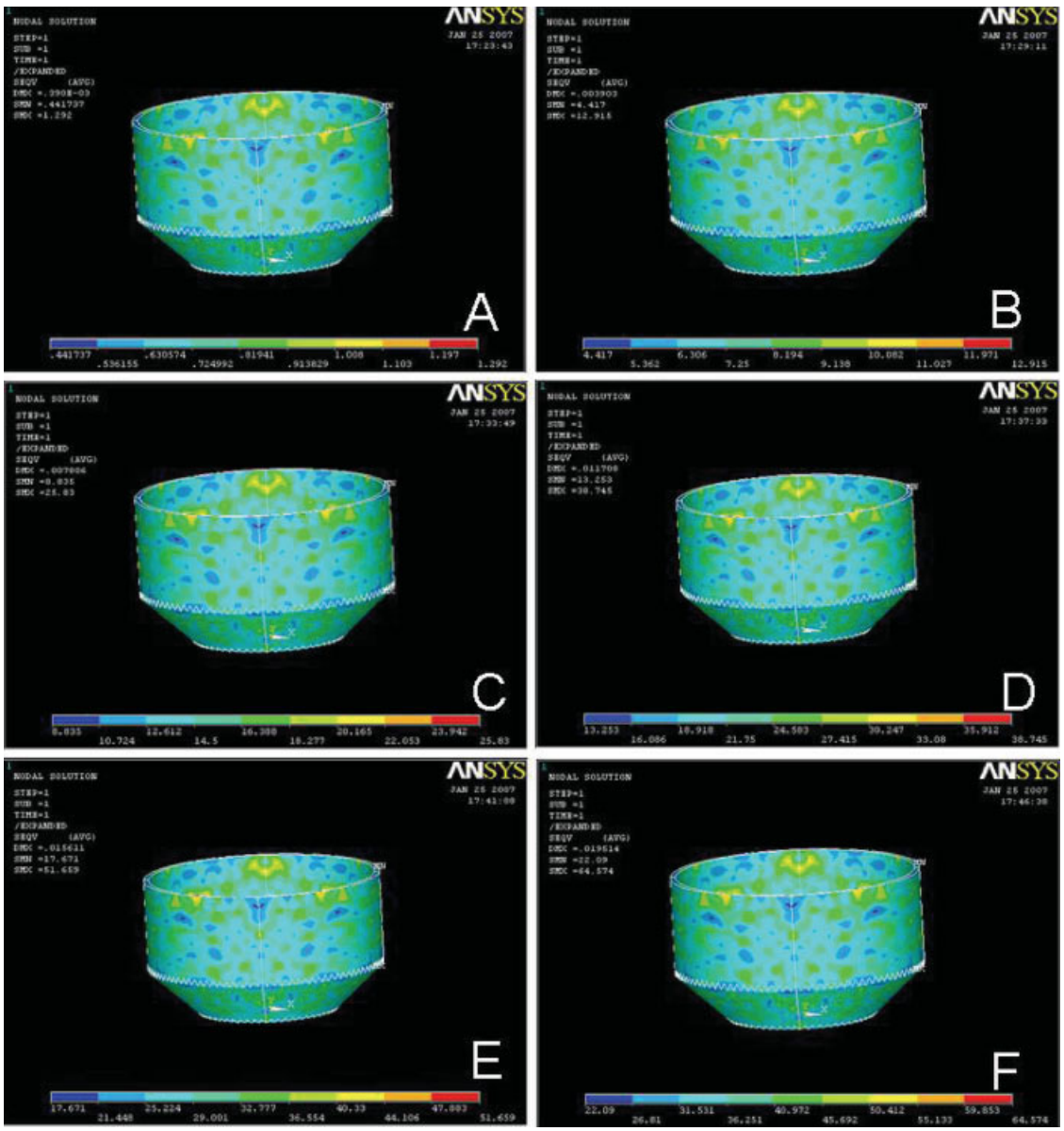

Figure 26 Pressure distribution on FRP component made by RPM technique where the rubber mold contains 75 phr carbon black. (Number inside parenthesis indicates applied pressure). (A) (1 MPa); (B) (10 MPa); (C) (20 MPa); (D) (30 MPa); (E) (40 MPa); (F) (50 MPa). [Color figure can be viewed in the online issue, which is available at www.interscience.wiley.com.]

eters; Ogden 2nd, 3rd orders; polynomial 1st, 2nd, 3rd orders; Yeoh 2nd, 3rd orders, Neo-Hooken, Arruda-Boyce fitted well with experimental data, 9 parameters Mooney-Rivlin strain energy density function is used to verify the stress-strain data. The nine parameters are given in Table V. Few representative plots for 0, 60, and 75 phr carbon black loading rubber mold are shown in Figures 24–26, respectively. It again proves that the pressure is uniformly distributed over the surface over the entire rage of hardness i.e., 50–85 shore A. Now to find out the optimum hardness of rubber mold, the transmitted pressure was plotted against applied pressure for various hardness of rubber mold and shown in Figure 27. It shows that 72 shore A hardness of the rubber mold (45 phr carbon black loading) is very good for RPM technique, where the distribution of pressure is excellent and transmitted pressure is $\sim$ 82%. No significant difference is observed for other vulcanizates i.e., A_0, A_{15}, A_{30}, A_{60}, and A_{70}. Why all these rubbers show same transmitted pressure except 72 shore A hardness of the rubber mold (45 phr carbon black loading) is not clear at this moment. A detailed investigation is required.

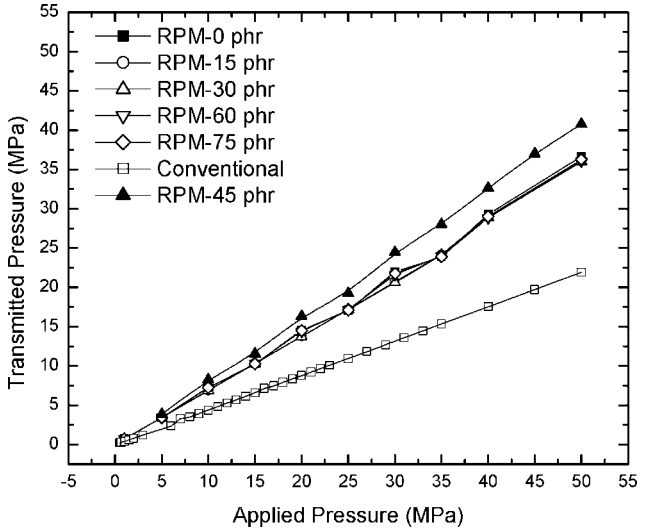

Figure 27 Transmitted pressure versus applied pressure for RPM technique where the loading of carbon black was varied from 0 to 75 phr and conventional technique.

CONCLUSIONS

The RPM technique is being developed to provide a low cost alternative for producing FRP composites. The natural rubber is used to exert hydrostatic pressure on the laminate during curing. The performance of RPM technique was analyzed by ANSYS using various strain energy density function of 2-, 3-, 5- 7-, and 9 parameter Mooney-Rivlin; 1st- 2nd- and 3rd order Ogden; Neo-Hookean; 1st-, 2nd-, and 3rd order Polynomial; Arruda-Boyce; 1st-, 2nd-, and 3rd order Yeoh; and Gent over a wide range of processing pressure i.e., 0.5–50 MPa and hardness of rubber mold 50–85 shore A. The following conclusions were made from this analysis:

1. Pressure is uniformly distributed over the complex shaped product in RPM technique compared to the conventional process.
2. 81–82% pressure is transmitted to the FRP component during processing whereas only 40–41% pressure in case of conventional process.
3. 45 phr black loading i.e., 72 shore A hardness of the rubber mold is appropriate to get a uniform pressure distribution over the complex shaped product.
4. The thickness of FRP component and vol % of fibers in composites do not affect the uniform pressure distribution on FRP component when it is made by RPM technique.
5. No significant difference in pressure distribution on FRP component is observed when the rubber molds are analyzed by 2-, 3-, 5- 7-, and 9 parameter Mooney-Rivlin; 1st- 2nd-, and 3rd order Ogden; Neo-Hookean; 1st-, 2nd-, and 3rd order Polynomial; Arruda-Boyce; 1st-, 2nd-, and 3rd order Yeoh; and Gent models.

References

1. Kelly, A.; Zweben C. Comprehensive Composite Materials, Vol. 2: Polymer Matrix Composites; Elsiver: New York, 2000.
2. Agrawal, B. D.; Broutman, L. J. Analysis and Performance of Fiber Composite; Wiley: New York, 1990.
3. Hollaway, L. Handbook of Polymer Composites for Engineering; Woodhead: Cambridge, England, 1994.
4. Edwards, K. L. Mater Des 1998, 19, 1.
5. Kumar, P. Elements of Fracture Mechanics; Wheeler: India, 1 999.
6. Wang, Z. J.; Liu, J. G.; Wang, X. Y.; Hu, Z. Y.; Guo, B. J Mater Process Technol 2004, 151, 80.
7. Kar, K. K.; Kumar, P.; Saha, T. K.; Sharma, S. D. Indian Pat. 2078/Del/2004 (2004).
8. Kar, K. K.; Sharma, S. D.; Behera, S. K.; Kumar, P. J Appl Polym Sci 2006, 101, 1095.
9. Kar, K. K.; Sharma, S. D.; Behera, S. K.; Kumar, P. Kautschuk Gummi Kuntstoffe 2006, 59, 169.
10. Kar, K. K.; Sharma, S. D.; Behera, S. K.; Kumar, P. J Elastomers Plast 2007, 39, 117.
11. Kar, K. K.; Sharma, S. D.; Behera, S. K.; Kumar, P. Curr Sci 2006, 90, 1452.
12. Kar, K. K.; Sharma, S. D.; Sah, T. K.; Kumar, P. J Reinforced Plast Compos 2007, 26, 269.
13. Sharma, S. D.; Kumar, P.; Kar, K. K. Compos Sci Technol, submitted.
14. Sharma, S. D.; Kumar, P.; Kar, K. K. Polymer Composites 2006, 90, 149.
15. Sharma, S. D.; Kumar, P.; Kar, K. K. J Compos Mater, submitted.
16. Sharma, S. D.; Kumar, P.; Kar, K. K. Polym Compos, submitted.
17. Shukla, M. Experimental and numerical investigation of induced distortions and stresses of angles composites during autoclave manufacturing; Indian Institute of Technology Kanpur: Kanpur, India, 2006; p 101.
18. Yeoh, O. H. Rubber Chem Technol 1993, 66, 754.
19. Boyce M. C.; Arruda, E. M. Rubber Chem Technol 2000, 73, 504.
20. Horgan, C. O.; Schwartz, J. G. J Mech Phys Solids 2005, 53, 545.
21. Bradley, G. L.; Chang, P. C.; Mckenna, G. B. J Appl Polym Sci 2001, 81, 837.
22. Yeoh, O. H. Rubber Chem Technol 1990, 63, 792.
23. Gent, A. N. Rubber Chem Technol 1996, 69, 59.